Miner Petrol (2013) 107:101–123
DOI 10.1007/s00710-012-0223-9

ORIGINAL PAPER

Origin and evolution of the Ilmeny–Vishnevogorsky carbonatites (Urals, Russia): insights from trace-element compositions, and Rb-Sr, Sm-Nd, U-Pb, Lu-Hf isotope data

I. L. Nedosekova · E. A. Belousova · V. V. Sharygin · B. V. Belyatsky · T. B. Bayanova

Received: 25 April 2011 / Accepted: 13 July 2012 / Published online: 5 August 2012

Abstract The carbonatites of the Ilmeny-Vishnevogorsky Alkaline Complex (IVAC) are specific in geological and geochemical aspects and differ by some characteristics from classic carbonatites of the zoned alkaline-ultramafic complexes. Geological, geochemical and isotopic data and comparison with relevant experimental systems show that the IVAC carbonatites are genetically related to miaskites, and seem to be formed as a result of separation of carbonatite liquid from a miaskitic magma. Appreciable role of a carbonate fluid is established at the later stages of carbonatite formation. The trace element contents in the IVAC carbonatites are similar to carbonatites of the ultramafic-alkaline complexes. The characteristic signatures of the IVAC carbonatites are a high Sr content, a slight depletion in Ba, Nb, Ta, Ti, Zr, and Hf, and enrichment in HREE in comparison with carbonatites of ultramafic-alkaline complexes. This testifies a specific nature of the IVAC carbonatites related to the fractionation of a miaskitic magma and to further Late Paleozoic metamorphism. Isotope data suggest a mantle source for IVAC carbonatites and indicate that moderately depleted mantle and enriched EMI-type components participated in magma generation. The lower crust could have been involved in the generation of the IVAC magma.

Editorial handling: O. Thalhammer

I. L. Nedosekova (✉)
UB RAS, AN Zavaritsky Institute of Geology and Geochemistry, Ekaterinburg, Russia
e-mail: vladi49@yandex.ru

E. A. Belousova
GEMOC ARC National Key Centre, Macquarie University, Sydney, Australia
e-mail: elena.belousova@mq.edu.au

V. V. Sharygin
VS Sobolev Institute of Geology and Mineralogy, SD RAS, Novosibirsk, Russia
e-mail: vsharygin@ngs.ru

B. V. Belyatsky
VNII Okeangeologia, St. Petersburg, Russia
e-mail: bbelyatsky@hotmail.ru

T. B. Bayanova
Institute of Geology KNC RAS, Apatity, Russia
e-mail: tamara@geoksc.apatity.ru

Introduction

The Ilmeny-Vishnevogorsky Alkaline Complex (IVAC) is one of the largest alkaline complexes containing miaskites, carbonatites, fenites and abundant rare metal—rare earth mineralization with large deposits of Nb, Zr and REE. This complex is situated in the Southern-Central Urals and has been known since the late 18th century. Miaskite (a variety of nepheline syenite) and a number of new minerals (ilmenite, monazite, aeschynite, cancrinite, chevkinite, pyrochlore) were firstly described there (Menge 1842; Rose 1839). Endogenic carbonate veins with pyrochlore mineralization have been discovered in the Vishnevogorsky miaskite massif after 1940 (Zhabin 1959). Over the next 50 years, more than 10 new deposits and occurrences of Nb and REE related to carbonatites of the IVAC were found (Fig. 1): Vishnevogorsky, Potanino, Byldym, Ishkul, Baidashevo, Uvildy, Svetlinskoe and others (Levin et al. 1997).

The carbonatites of the IVAC are specific in geological and geochemical aspects and differ from classic carbonatites of the ring alkaline-ultramafic complexes. These differences provoked long debates on whether these carbonate rocks belong to carbonatites (Ginzburg and Samoilov 1983; Bagdasarov 1990; Egorov 1990; Sokolov 1991 and others). The most debatable questions for the IVAC are: (1) the

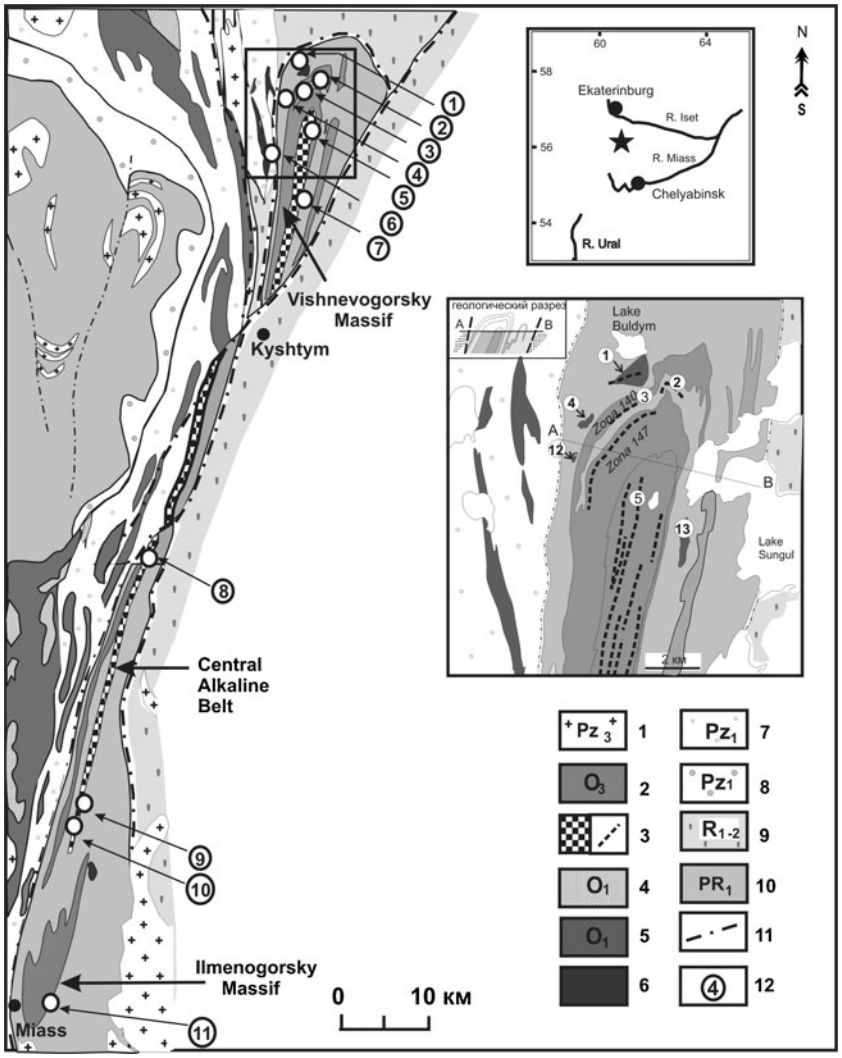

Fig. 1 Geological scheme of the Ilmeny-Vishnevogorsk alkaline complex modified after Levin et al. (1997) and Zoloev et al. (2004). *1* – granite (PZ_3 - Late Paleozoic); 2-3 – IVAC: *2* – miaskites of the Vishnevogorsk and Ilmenogorsk plutons; *3* – zones of carbonatites and carbonate-silicate rocks; *4* – gabbros of ophiolitic complex (O_1 - Early Ordovician); *5* – ultramafic rocks of ophiolitic complex (O_1); *6* – meta-ultramafic rocks of the Buldym, Kagan, and Nyashevo complexes (PR_1 - Paleoproterozoic ?); *7* – volcanosedimentary rocks of the Tagil-Magnitogorsk megasynclinorium (Pz_1); *8* – garnet-mica schists and eclogites of the eastern Ufalei complex (Pz_1- Early Paleozoic); *9* – plagioschists and quartzites of the Sysert-Ilmenogorsk complex (R - Riphean); *10* – plagiogneisses, granitic migmatites, crystalline schists, amphibolites, and quartzites of the Sysert-Ilmenogorsk and Ufalei complexes; *11* – faults and unconformities; *12* – Nb and REE deposits and carbonatite occurrences (figures in circles): *1* – Buldym (Nb and REE); 2-3 –Vishnevogorsk (Nb): *2* – Zone 125; *3* – Zone 140, Vishevogorsky miaskite satellite saddle-shaped body; *4* – Spirikha (REE); *5* – Svetlinskoe (Nb); *6* – Kagan (REE); *7* – Potanino (Nb); *8* – Uvildy (Nb); *9* – Baidashevo (Nb); *10* – Ishkul (Nb); *11* – Ilmeny, mine 97 (Nb and REE); *12* – Khalkhidino; *13* – Sungul

direct spatial and genetic relations of carbonate rocks with nepheline syenites and fenite zones; and (2) the absence of ijolite-urtite rock series like in classic alkaline-ultramafic complexes. It also emphasizes the derivation of the IVAC and the question of parental magmas, i.e. whether the silicate alkaline rocks and related carbonatites are differentiates of alkaline-ultramafic magmas, or products of an independent miaskitic magma. Furthermore, the fact that the IVAC carbonatites occur as veins, stockworks and metasomatic zones, independent of the composition of the country rocks, and the lack of typical magmatic, mono-stage features, may indicate that silicate-carbonate immiscibility and fluids played an important role in the origin of the IVAC carbonatites.

Two diverging hypotheses were postulated for the origin of the miaskites: a) miaskites and carbonatites represent crystallization products of deep-seated alkaline magmas (Kononova et al. 1979), or b) they are the result of metasomatism and subsequent anatexis of crustal material (i.e. crustal palingenesis; Ronenson 1966). According to the model of crustal anatexis (Ronenson 1966; Levin et al. 1997) the IVAC was formed under the influence of a

powerful flow of juvenile alkaline hydrous-carbon dioxide fluids onto the gneiss–amphibolite protolith of the Sysert–Ilmenogorsky Block and subsequent development of crustal anatexis controlling the formation of carbonatite–miaskite intrusions. However, the low primary Sr isotope ratio (i.e. $^{87}Sr/^{86}Sr \sim 0.703$) and the oxygen isotope composition (i.e. $\delta^{18}O$ from +5.4 to +7.6‰) suggest that the IVAC miaskites, like those from classic alkaline-ultramafic complexes, derived from deep-seated (possible mantle) melts. Palingenesis is supposed to play a minor role (Kononova et al. 1979; Kramm et al. 1983; Chernyshev et al. 1987).

The Sr, C, O and S isotopic compositions of the IVAC carbonatite veins also indicate a deep-seated, possibly mantle source, which justifies their classification as carbonatites (Kononova et al. 1979). Geological-geochemical peculiarities of the IVAC carbonatites allow a further classification into "carbonatites related to nepheline syenites and zones of alkaline metasomatic rocks" (Borodin 1966, 1994; Ginzburg and Samoilov 1983), and "carbonatites of linear fracture zones" (Bagdasarov 1979).

New Rb-Sr, Sm-Nd, U-Pb, Lu-Hf isotopic and ICP-MS geochemical data, obtained during this study, will provide a better understanding of the origin of the IVAC, the timing and formation of carbonatites and ores, their sources, the role of metamorphic processes, the geochemical evolution of the complex and genetic relations to carbonatites associated with alkaline ultramafic rocks.

Geological setting and composition of the Ilmeny-Vishnevogorsky Alkaline Complex

The IVAC (Southern-Central Urals) is located in the centre of the large metamorphic Sysert-Ilmenogorsky anticlinorium. This metamorphic complex consists of two structural units and is characterized by a long geological history. Its core (the lower structural unit) is composed of retrograde gneisses, granulites and migmatites of the Selyankino Suite (U-Pb zircon age 1,820±70 Ma, Tugarinov et al. 1970) and plagiogneisses and amphibolites of the Vishnevogorsky Suite (PR_1). The upper structural unit comprises the Ilmenogorsky Suite in the south and the Shumikhino Suite in the north. This section is represented by amphibolites, plagiogneisses, crystalline schists and quartzites. It is suggested that rocks of this structural unit are pre-Uralides (rift-related?) metamorphic complexes with an U-Pb age interval from 643 ±46 Ma (Ilmenogorsky Suite) to 576±65 Ma (Shumikhino Suite) (Krasnobaev and Davydov 2000). All stratigraphic units of the Sysert-Ilmenogorsky anticlinorium (except the oldest Selyankino and Firsov Suites) contain abundant lense-like boudinaged bodies of ultramafic rocks, comprised by metamorphosed olivinites (metadunites) and metaperidotites (amphibolite facies olivine-enstatite and olivine-enstatite-antophyllite assemblages, Varlakov et al. 1998). The overlying Riphean schists and quartzites belong to the sedimentary cover. The U-Pb and Rb-Sr ages of crystallization of silicate rocks and carbonatites of the IVAC occurring in the centre of the Sysert-Ilmenogorsky anticlinorium are 434±15 and 446± 12 Ma, respectively (Kramm et al. 1983, 1993). The subsequent metamorphism and granite formation in the Sysert-Ilmenogorsky anticlinorium are related to the Hercynian orogeny (360–320 Ma) and post-collision extension (260–240 Ma).

The IVAC extends from north to south for more than 150 km with a maximum width of 4–6 km (Fig. 1), and consists of two miaskite plutons (20–25×6 km), the Vishnevogorsky and the Ilmenogorsky pluton, which are connected by the 150 km Central Alkaline Belt (width–20 km), composed of fenites, feldspathic metasomatic rocks, miaskites, melanocratic carbonate-silicate rocks and carbonatites.

The Vishnevogorsky and Ilmenogorsky plutons mainly consist of miaskites and subordinate amphibole miaskites, plagiomiaskites and alkali syenites of the contact facies. Miaskites contain microcline-perthite (up to 50 vol %), oligoclase (up to 12 vol %), nepheline (up to 28–35 vol %) and lepidomelane (up to 30 vol %) (Levin et al. 1997). Calcite (up to 5–10 vol %) is quite abundant in the Vishnevogorsky miaskites. Zircon, ilmenite, magnetite, titanite, pyrochlore, and apatite are minor and accessory minerals. Secondary minerals are albite, cancrinite, sodalite, analcime, natrolite, and sericite. Banding, some of which is gneissic and vague banding of unknown origin, is a common feature of most miaskites and is related to the Late Paleozoic metamorphism (Kononova et al. 1979). Massive miaskites occur occasionally and belong to a magmatic stage of crystallization. The magmatic origin of miaskites is confirmed by its relatively stable modal composition corresponding to eutectic crystallization, sharp intrusive contacts with country rocks, and the occurrence of veined miaskitic aplites and pegmatites. Bands of melanocratic carbonate-silicate rocks and sheet-like bodies of carbonatites extend parallel to the intrusive contacts in the apical part of the Vishnevogorsk pluton and in miaskites of the Central Alkaline Belt. Unlike the miaskites of the Vishnevogorsky and Ilmenogorsky plutons, miaskites of the Central Alkaline Belt are rich in antiperthite and poor in nepheline (24–26 vol %). They contain oligoclase with spindle-shaped ingrowths of K-feldspar or pure albite with sporadic K-feldspar ingrowths. Miaskite bodies of the Central Alkaline Belt are mylonitized and schistose.

Miaskite intrusions are surrounded by pyroxene fenites at conformable contacts and by biotite and amphibole-biotite fenites at crosscutting contacts. Fenites are also abundant in the Central Alkaline Belt. Fenites are characterised by presence of the following minor or accessory minerals: titanite,

ilmenite, apatite, ilmenorutile, zircon, allanite, chevkinite, molybdenite, pyrrhotite, pyrite and magnetite.

Carbonatite occurrences

Carbonatites are most abundant in the northern part of the IVAC in the apical part and exocontact aureole of the Vishnevogorsky miaskite pluton and in the Central Alkaline Belt. Exocontact carbonatites are located in fenitized rocks of the Vishnevogorsky Suite and in ultramafic bodies near the NW contact of the Vishnevogorsky intrusion—i.e. at Buldym, Spirikhino, Haldichino, Sungul (Fig. 1). Carbonatites are extremely rare in the southern IVAC. In the Ilmenogorsky Massif they occur as rare individual veins in miaskites and in the eastern exocontact in an ultramafic body (Polyakov and Nedosekova 1990). The largest and most abundant occurrences of carbonatites are situated in the endo- and exocontact areas of the Vishnevogorsky pluton (Fig. 1). Sheet-like bodies and veins of carbonatites form two essential zones in the northern part of the pluton: zone 147 (width–up to 30 m, extension–up to 4 km) and zone 140 (extension–up to 1.7 km). The zone 140 represents a series of subparallel veins (from 10 cm to 7–10 m in thickness) of carbonatite, albitites and miaskitic pegmatites confined to the contact of fenites and miaskites of the Vishevogorsky satellite saddle-shaped body. In addition, abundant carbonate veins occur in the fenite aureole of the Vishnevogorsky intrusion, within amphibolites and plagiogneisses of the Vishnevorsky Suite.

Carbonatites are also abundant in the Central Alkaline Belt (Potanino, Ishkul, Baydashevo, Uvildy, Svetlinskoe Nb occurrences, Fig. 1). The Potanino Nb deposit is one of largest occurrences and confined to the eastern contact with country rocks. There carbonatites form a linear stockwork zone in miaskites and fenites (thickness–40 m, extension–up to 15 km).

Miaskite-related carbonatites (Vishnevogorsky and Potanino) are represented by early and late calico-carbonatites (sövite I and sövite II). Sövite I forms schlieren and bed-like bodies or dikes (thickness – up to 10 m, extension - up to some hundred meters) conformable with the layering in the miaskite as well as to the contact of the miaskite intrusion. Massive types are common. Some sövite I dikes and veins (thickness – 0.5–1 m) are brecciated and bear rounded fragments (1–5 cm), both of miaskites and their pegmatites and individual large grains of miaskitic minerals “cemented” by calcite-silicate fine-grained groundmass. In the contact with fenites, the carbonatites may contain their debris. The sövite I consists of calcite, biotite, K-feldspar, nepheline, apatite and minor/accessory pyrochlore, uranpyrochlore, zircon, ilmenite, magnetite, pyrrhotite, pyrite. Sövite II forms pockets and veins in early sövite I and in miaskites and their pegmatites, sometimes cutting early carbonatites. They comprise calcite, biotite, apatite, pyrochlore, zircon, ilmenite, pyrrhotite and pyrite.

Carbonatites from the exocontact aureole of the miaskite plutons and the Central Alkaline Belt form stockworks, veined and lens-like bodies and metasomatic zones. They are coarse-grained types and contain fragments of fenites and calcite, clinopyroxene, feldspars, phlogopite, pyrochlore, titanite, apatite, ilmenite, chevkinite, orthite, zircon, magnetite, pyrrhotite and pyrite.

The Buldym carbonatites are localized in the Buldym ultramafic massif, 100 m north of the Vishnevogorsky pluton (Fig. 1). They form linear carbonatite bodies up to 10 m in thickness and hundreds of meters in extent, controlled by NE-trending faults dipping to the northwest and accompanied by thick carbonate-phlogopite-richterite metasomatic zones (fenite replacing ultramafic protolith). The total thickness of carbonatites and associated metasomatic rocks reaches 50 m. The Buldym carbonatites are represented by dolomite-calcite carbonatite (Sövite III) and late dolomite carbonatite (Beforsite IV). Sövite III is a massive coarse-grained rock containing dolomite, calcite, tetraferriphlogopite, richterite, and minor/accessory pyrochlore, zircon, magnetite, ilmenite, pyrrhotite, and pyrite. Beforsite IV occurs as thin veins consisting of dolomite, monazite, aeschynite, REE-bearing pyrochlore, fersmite, and phlogopite replaced by chlorite, winchite, apatite, magnetite, ilmenite, zircon, and occasional strontianite

Analytical methods

Chemical analyses of whole rocks for major oxides were performed at the Institute of Geology and Geochemistry (IGG) of the Ural Division of the Russian Academy of Sciences in Yekaterinburg. Trace element (35 elements) compositions of the studied rocks and minerals were determined by acid decomposition of the samples and subsequent analysis on high-resolution ICP-MS Element 2. The uncertainty of element analysis is no higher than 8–10 % for concentrations 10–20 times above the detection limit.

Sr and Nd isotope compositions and concentrations in carbonates were also determined at the IGG. Prepared samples were decomposed with 3 % CH_3COOH in a Teflon beaker at room temperature. Chromatographic extraction of Sr was carried out with AG-50×8 (200–400 mesh) resin. Neodymium was separated during two stages: in the first stage total REE were isolated by stepwise elution on cationite AG-50×8 (200–400 mesh), and then by extraction chromatography on columns filled with KEL-F powder coated by ionite (HDEHP). The isotopic composition was measured on a Finnigan MAT-262 multicollector solid-phase mass spectrometer in the static regime. The measured

$^{87}Sr/^{86}Sr$ and $^{143}Nd/^{144}Nd$ ratios were normalized to $^{86}Sr/^{88}Sr=0.1194$ and $^{146}Nd/^{144}Nd=0.7219$, correspondingly. External uncertainty and reproducibility were controlled by systematic measurements of LaJolla and MTI international standards. The blank contamination for Sr and Nd was as low as 70 and 90 pg, respectively.

Nd and Sm isotopic compositions of the studied minerals and whole-rocks samples of the Buldym Massif were measured on a multicollector Finnigan MAT-262 (RPQ) solid-phase mass spectrometer in the static regime at the Geological Institute of the Kola Center of the Russian Academy of Sciences (Apatity). The measured ratios were normalized to $^{148}Nd/^{144}Nd=0.241570$ and then recalculated to $^{143}Nd/^{144}Nd=0.511833$ in the LaJolla standard. Over the period of measurements, the average $^{143}Nd/^{144}Nd$ values for LaJolla ($n=11$) and JNdl ($n=44$) were 0.511833±6 and 0.512074±8 (2σ), respectively. The blank level for Nd and Sm during analysis was 0.3 and 0.06 ng, respectively.

Carbon and oxygen isotopic compositions of carbonates were determined at the Analytical Center of the Far East Geological Institute of the Russian Academy of Sciences in Vladivostok. The samples were prepared using the McCrea technique. Carbon dioxide was extracted from carbonates with 100 % phosphoric acid. The reaction proceeded in vacuum at a temperature of 50 °C. The obtained CO_2 was refined from impurities in a cryogenic trap. The C and O isotope ratios were measured on a Finnigan MAT-252 mass spectrometer using a double system of bleeding. The weight of analyzed samples was 2–5 mg. The reproducibility of $\delta^{18}O$ and $\delta^{13}C$ (1σ) determinations was 0.1‰ and 0.05‰, respectively ($n=5$). Calibration of analytical procedure was carried out using the NBS-18, NBS-19, and IAEA-CO-8 international standards.

IVAC zircon Lu-Hf- and U-Pb-isotope compositions were studied by laser ablation at the GEMOC (Macquarie University, Sydney). Hf isotope composition and U-Pb–dating was conducted by UV laser UP213 New Wave (Merchantek) coupled with a MC-ICP MS Nu-Plasma and Agilent 7000 ICP MS instrument. Analyses were done with a laser beam size of about 50 μm. Ablation time was about 100–120 s, laser pit depth was 40–60 μm. Errors of values for the $^{176}Hf/^{177}Hf$ ratio are ±0.00002 (2σ), which is equal to ±0.7 εHf based on zircon standard no. 91500. The principal of U-Pb dating and analysis of Hf isotope composition were described in detail previously (Griffin et al. 2000).

Major and trace elements in the IVAC carbonatites

The representative chemical compositions of carbonatites from different occurrences of the IVAC are given in Table 1. Chemical compositions of carbonatites are shown in Fig. 2. The contents of major elements indicate ranges from calcio- (sövites) and magnesiocarbonatites (beforsites). The tendency to ferrocarbonatite compositions is noted among sövites I due to local enrichment of these rocks in ilmenite, pyrrhotite, and pyrite, whereas the composition of carbonates remains unchanged. Carbonatites of the Vishnevogorsky pluton and the Central Alkaline Belt (the Potanino and Uvildy occurrences) are located in the calico-carbonatite compositional field forming separate areas (for sövite I and II) in the Wooley and Kempe (1989) CaO-MgO-FeO classification diagram (Fig. 2a). Sövite I differs from sovite II in higher contents of MgO (0.5–4.2 wt %), $A1_2O_3$ (2.0–4.6 wt %) and SiO_2 (5–12 wt %). Sövite II is characterized by appreciable MnO (0.42–0.77 wt %).

Carbonatites from the Buldym and Baidashevo occurrences make up individual fields in the classification diagram CaO-MgO-FeO after Wooley and Kempe (1989) and differ from carbonatites of the Vishnevogorsky pluton and the Central Alkaline Belt as well. The early dolomite-calcite carbonatite corresponds to calico-carbonatite (sövite III) in chemical composition, and the late dolomite carbonatite is close to magnesio-carbonatite (beforsite IV). They differ from carbonatites of the aforementioned deposits in high contents of MnO (1.1–1.4 wt %) and MgO (5.6–7.2 wt % in dolomite-calcite carbonatite).

The position of averaged compositions of the IVAC carbonatites in the CaO-MgO-FeO diagram illustrates a similar compositional trend, common to carbonatite-related complexes worldwide: from calico-carbonatite to magnesio-carbonatite. Unlike carbonatites of highly evolved complexes such as Tomtor, Chilva, Gudini, Mud Tank and others, the IVAC rocks do not show a pronounced tendency to ferro-carbonatite composition (Fig. 2b). The REE and rare element contents for carbonatites of the IVAC are presented in Table 1 and in Fig. 3 a, b. All carbonatite of the IVAC are characterized by high contents of Sr (11,000–23,000), Ba (300–3,400) and REE (1,500–3,200 ppm) and wide variations in contents of Nb (up to 1,500), Zr (up to 100), V (up to 135) and Th (up to 1,400 ppm) (Nedosekova et al. 2009), comparable with averaged compositions of calcio- and magnesio-carbonatites worldwide (Wooley and Kempe 1989).

Carbonatite I (Sövite I) is characterized by high Sr (3,950–12,340 ppm), Ba (700–3,400 ppm) and ∑REE (700–1,600 ppm) contents but lower than sövite II, which is typical for high-temperature and magmatic carbonatites. The Nb/Ta ratios are between 11 and 98 (mean 43) and are quite similar to those for magmatic carbonatites. The Sr/Ba ratios are high (17–21 ppm), typical for the high-temperature deep facies of carbonatites (Bagdasarov 1994). The Eu/Eu* ratio (0.98–0.91) is maximal and close to that of miaskite, confirming that the early generation of carbonatites belongs to high-temperature derivatives of miaskitic magma.

Table 1 Representative chemical composition of carbonatites from IVAC

	Sövite I				Sövite II Vein			Sövite III Vein			Beforsite IV Vein	
	Sheet		Brechia Dyke									
Weight percent												
SiO_2	4.65	22.88	13.02	24.00	3.38	9.72	11.86	1.00	7.40	3.61	0.72	30.50
TiO_2	0.4	0.38	2.1	2.61	0.01	0.65	0.15	0.01	0.07	0.02	0.18	0.11
Al_2O_3	1.23	8.71	4.57	7.66	0.26	3.15	3.18	0.03	1.4	0.73	0.02	1.29
Fe_2O_3	0.01	0.17	0.01	1.20	0.14	0.05	0.75	0.3	0.79	0.34	0.34	1.96
FeO	1.07	3.0	7.3	5.6	1.4	5.8	5.3	2.03	2.1	1.6	3.0	1.0
MnO	0.26	0.25	0.31	0.25	0.28	0.49	0.38	1.3	1.1	1.2	1.40	0.21
MgO	0.22	1.54	2.93	4.6	0.2	0.83	0.7	5.39	7.26	5.6	17.60	25.5
CaO	54	33.36	41.26	25.5	54.56	45.0	48.2	48.8	43.85	48.0	33.12	17.91
Na_2O	0.6	2.5	0.9	1.5	0.7	1.0	2.18	0.2	0.6	0.20	0.15	0.70
K_2O	0.75	4.32	3.36	5.01	0.07	1.6	1.66	0.02	1.09	0.68	0.01	0.01
P_2O_5	0.02	0.79	2.45	0.03	0.51	2.07	1.24	0.01	0.01	0.01	0.18	1.35
S		1.2		0.20	0.90	0.82	1.30					
LOI	36.6	19.4	19.8	20.6	36	27.85	23.0	40.8	34.3	38.0	43.15	17.8
total	99.81	98.5	98.01	98.76	98.41	99.03	99.9	99.89	99.97	99.97	99.87	98.34
ppm												
Li	2	3	10	16	4	8.2	7	0.45	18	12	0.1	3
Rb	15	52	120	152	2	38	62	0.3	52	44	0.4	0.1
Be	0.1	0.4	0.8	0.6	0.9	0.7	0.8	0.05	1.3	0.3	0.5	0.6
Sr	8,355	9,247	3,953	3,946	10,973	9,114	11,530	12,223	9,547	10,279	6,611	3,796
Ba	700	3,054	3,405	1,901	266	1,060	790	540	484	224	233	302
Sc	3	3	4	0.5	11		5	3	6	2	1	2
V	3	61	239	212	104	76	104	3	67	15	8	51
Cr	8	25	53	40	15	16	15	14	138	107	23	35
Co	2	4	20	19	2	16	13	23	7	5	16	7
Ni	12	11	16	34	13	12	23	68	13	10	13	30
Cu	24	15	21	11	12	20	24	30	24	24	20	24
Zn	5	32	174	161	22	92	36	171	88	49	47	8
Y	115	98	61	42	113	100	90	87	62	69	93	74
Nb	36	57	123	153	40	352	1,600	4	930	20	88	15
Ta	0.3	1.7	10.9	11	1.2	4	7	0.01	1.2	0.02	0.1	0.1
Zr	2.2	109	21	5	36	25	31	0.11	42	2	24	37
Hf	0.1	1.2	0.8	0.2	2	1	1	0.16	0.5	0.1	0.4	0.5
Mo	0.1	0.3	0.1	0.3	0.2	0.33	1	0.46	0.6	0.6	1.2	0.0

Table 1 (continued)

	Sövite I				Sövite II Vein			Sövite III Vein			Beforsite IV Vein	
	Sheet		Brechia Dyke									
Pb	6	5	4	4	116	18	32	30	23	14	23	59
Th	0.5	3	2	0.9	0.6	12	18	1.0	22	3	681	1,418
U	0.1	1	0.4	3	2	11	26					
La	430	370	191	147	425	356	390	428	577	598	2,285	18,959
Ce	520	641	394	287	838	740	733	1,385	1,022	1,056	4,092	25,500
Pr	94	70	56	36	77	96	69	58	58	59	180	913
Nd	290	221	211	130	245	356	238	222	180	202	543	2,273
Sm	46	31	31	19	41	43	41	51	38	41	70	168
Eu	14	9	10	6	10	13	12	13	10	11	34	28
Gd	48	25	29	14	43	41	39	41	28	32	65	87
Tb	4.0	3.0	2.7	1.8	4.7	4.8	4.2	6	4.3	5	10	11
Dy	28	15	14	10	28	26	22	34	23	25	60	46
Ho	3.7	3.1	2.5	1.9	5.9	4.8	4.3	7	5.0	5.5	11	7
Er	17.2	8.0	5.9	5.3	18	13	12	21	14	16	23	12
Tm	2.7	1.1	0.7	0.7	2.8	1.87	1.72	3	2.2	2.4	3.0	1.3
Yb	19	7	4.1	4.6	19	10.3	11.1	25	15	17	16	6
Lu	3.11	1	0.6	0.7	2.8	1.5	1.6	4.1	2.4	2.6	2	0.8
ΣTR + Y	1,635	1,504	1,013	706	1,874	1,808	1,588	2,384	2,043	2,595	7,487	48,087
TR_{Ce}/TR_{Y}	9	8	7	8	7	8	8	9	12	11	25	195
La/Yb	23	53	46	32	23	34	35	17	37	35	139	3,160
Y/Ho	31	32	24	22	19	21	20	13	12	13	8	11
Eu/Eu*	0.91	0.95	0.96	0.98	0.71	0.85	0.89	0.85	0.87	0.87	1.54	0.66

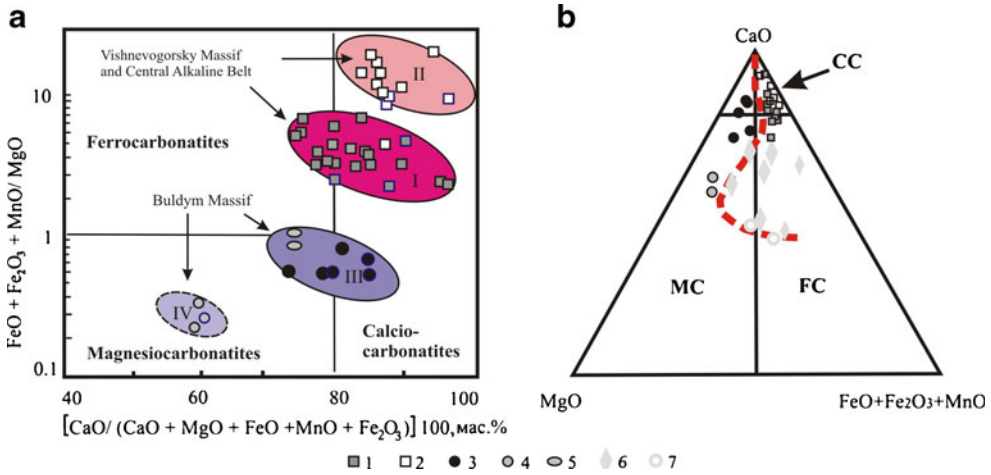

Fig. 2 Compositions of the IVAC carbonatites (wt %) on classification diagrams. **a** – Diagram from Wooley and Kempe (1989); **b** – Diagram from Gittnis and Harmer (1997). *1* – Sövite I, Central Alkaline Belt, Vishnevogorsky and Ilmeny Massifs; *2* – Sövite II, Central Alkaline Belt and Vishnevogorsky Massif; *3* – Sövite III, Buldym Massif; *4* – Beforsite IV, Buldym Massif; *5* – Sövite III, Baidashevo; 6-7 – Carbonatites of differentiated complexes: *6* – Tomtor; *7* – Gudini. Dashed line – trend for the Tomtor massif (Kravchenko et al. 2003). *CC* calciocarbonatites (sövites); *MC* magnesiocarbonatites; *FC* ferrocarbonatites. Authors' data for the IVAC carbonatite compositions with SiO_2<12 wt % were supplemented by the data from Levin et al. (1997)

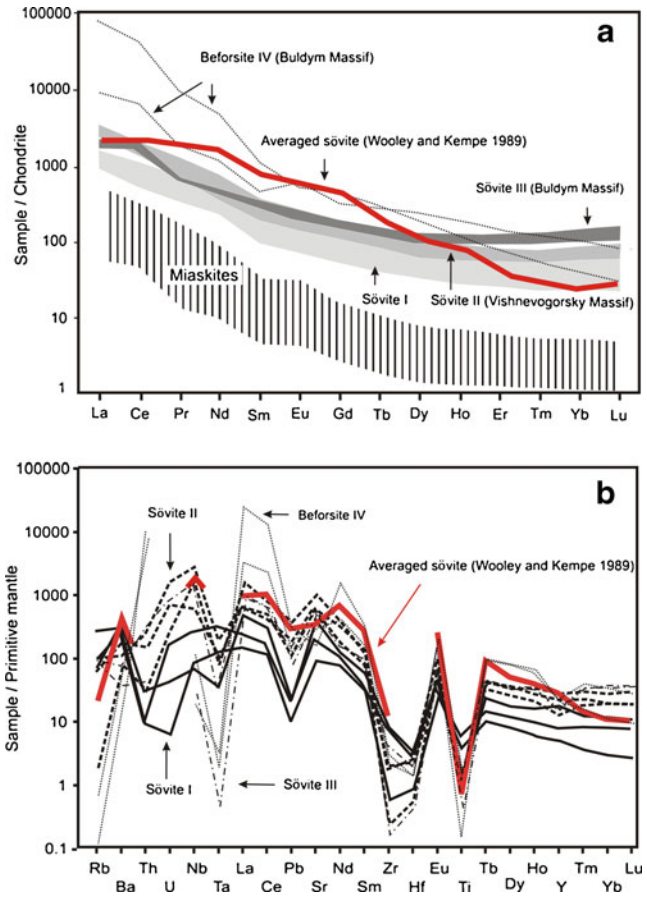

Fig. 3 Chondrite-normalized REE patterns (**a**) and primitive mantle-normalized trace element (**b**) diagrams for the IVAC carbonatites and miaskites (whole rock samples). Chondrite (C1) and primitive mantle values are from Sun and McDonough (1989). Average sövite is from Wooley and Kempe (1989)

Carbonatite II (Sövite II) is distinguished by the highest Sr (9,100–21,980 ppm) and REE (1,600–3,210 ppm) contents, high Nb/Ta (582–1,310) and Sr/Ba (78) ratios, and decrease in the Eu/Eu* ratio down to 0.70, which is typical for the late high-temperature carbonatite series (Samoilov and Smirnova 1980).

Dolomite-calcite carbonatites III (Sövite III) from the Buldym Massif are characterized by a similar Sr content and higher Nb, REE, Mn and HREE contents, compared to those of Carbonatite I from the Vishnevogorsky Massif (Nedosekova 2007a). Their REE patterns (Fig. 3a) are distinguished by elevated HREE contents and the lowest La/Yb ratio (17–37).

Dolomite carbonatites IV (Beforsite IV) from the Buldym Massif have extremely high REE (up to 48,000 ppm) and Th (up to 1,400 ppm) contents, due to the presence of minerals such as monazite and aeschynite, and are characterized by low Sr, Ba, and Nb contents in combination with the highest and variable Nb/Ta, Zr/Hf, Sr/Ba, and LREE/HREE ratios, typical for low-temperature members of carbonatite series. The lowest Eu/Eu* ratio (0.65) confirms that these rocks belong to the final stages of carbonatite generation.

Discussion

Geochemical evolution and comparative characteristics of the IVAC carbonatites

All calico-carbonatites of the IVAC are enriched in Sr (up to 4,000 ppm in Carbonatite I and 21,980 ppm in Carbonatite II) compared to carbonatites from ultramafic-alkaline-carbonatite ring complexes of platform (Fig. 4a). In the early high-temperature carbonatites of these complexes the

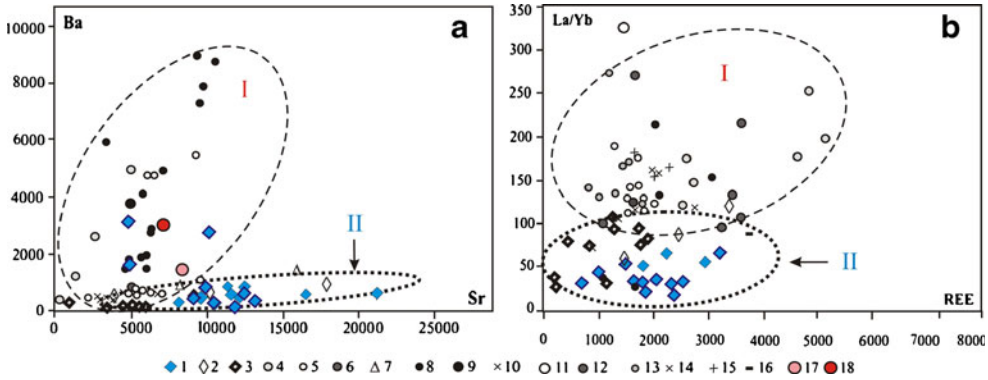

Fig. 4 Sr vs. Ba and La/Yb vs. REE diagrams for carbonatites related to alkaline ultramafic rocks (I) and linear fracture zones (II). 1-3 – Calico-carbonatites related to linear fracture zones: *1* – IVAC; *2* – Chernigovka; *3* – Penchenga (Glevassky and Krivdik 1981; Samoilov 1984; Samoilov and Ronenson 1987; Bagdasarov 1990; Vrublevsky et al. 2003; Rass et al. 2006; Nedosekova 2007a; 2007b; Nedosekova et al. 2009); *4-10* – Calciocarbonatites related to alkaline ultramafic complexes: *4* – Tomtor; *5* – Kola-Karelian Province; *6* – Fen; *7* – Oka, *8* – East African Province, *9* – West African Province; *10* – Eastern Sayan Complex; *11* – Oldoinyo Lengai; *12* – Kenya; *13* – Maimecha-Kotui Province; *14* – East Siberia Province; *15* – Aldan Province; *16* – Amba Dongan, India (Samoilov and Smirnova 1980; Samoilov 1984; Kravchenko et al. 2003; Wall and Zaitsev 2004; Oktyabr'sky et al. 2004); *17* – Averaged calico-carbonatite (Le Bas 1999); *18* – Average calico-carbonatite (Wooley and Kempe 1989)

average Sr content is about 5,800 ppm. The elevated Sr/Ba ratio (17–78) of the IVAC calico-carbonatites is typical for the high-temperature deep carbonatite facies and contrasts with volcanic carbonatites, where the Sr/Ba value is 1.2–2.6 (Samoilov 1984). From the early Carbonatites I to the late Carbonatites II the Ba/Sr ratio decreases with a decrease of Ba contents. Dolomite carbonatite IV of the IVAC is evidently depleted in Sr (3,790–6,610 ppm) and Ba (220–300 ppm) relatively to calico-carbonatites, apparently, because Sr is accumulated at the early stages of carbonatite formation, in contrast to alkaline ultramafic complexes, where the highest Sr and Ba contents are characteristics of the late generation of carbonatite.

Carbonatites of the IVAC are depleted in Nb and Ta (4–1,600 and 0.01–11 ppm, respectively) in comparison with carbonatites of the ultramafic-alkaline carbonatite complexes (which contain up to 4 wt % Nb and up to 0.2 wt % Ta) and high Nb/Ta ratio (66–1,310) with a maximum in pyrochlore-bearing varieties. In Carbonatites I Nb/Ta is 9–98, with a mean of 43 (Levin et al. 1997), i.e. close to the ratio in magmatic carbonatites (Bagdasarov 1994). The Nb/Ta ratio in Carbonatites II is much higher (217–1,310). Such an increase in the Nb/Ta ratio from early to late members of carbonatite series was already noted for ultramafic-alkaline-carbonatite complexes by Kukharenko et al. (1965). High and variable Nb/Ta ratios are characteristic of post-magmatic hydrothermal processes.

Zirconium (0.1–110 ppm) and Hf (0.1–1.0 ppm) contents in carbonatites of the IVAC are somewhat lower than in carbonatites of ultramafic-alkaline complexes. The Zr/Hf ratio varies from 18 to 92, i.e. from chondrite to suprachondrite values, and is close to high-temperature carbonatites and alkaline rocks (Fabio et al. 2002). It is also typical for other highly evolved and fluid-saturated magmatic systems (Bau 1996). In general, carbonatites of the IVAC show two correlation trends between the Zr content and the Zr/Hf ratio (Fig. 5a), clearly indicating a formation in the course of magma fractionation. The first trend is shown by carbonatites and miaskites of the Vishnevogorsky Massif and Central Alkaline Belt, whereas a second trend is indicated by carbonatites of the Buldym Massif and fenites of the Vishnevogorsky Massif. Carbonatites and miaskites of the Vishnevogorsky Massif are characterized by an almost linear decrease of Zr content and Zr/Hf ratios, illustrated by the first trend in Fig. 5a, starting from the miaskites to early carbonatites and trending further to the late carbonatites. This provides further evidence for differentiation and corresponds well with the Zr and Hf evolution trends of plumasite silicate magmas (Zaraysky 2005).

All calico-carbonatites of the IVAC are characterized by an enrichment of LREE relatively to HREE (LREE/HREE= 7–25), a feature seen in typical ultramafic-alkaline complexes. At the same time, carbonatites of the IVAC are slightly enriched in HREE, and the La/Yb ratio of these rocks (14–67) is markedly lower than that of carbonatites related to ultramafic-alkaline complexes (La/Yb=75–256) (Fig. 4b). Only volcanic carbonatite complexes of the East African Rift have a similarly low La/Yb ratio (28–41) (Samoilov and Smirnova 1980). Low La/Yb ratio is also characteristic for other carbonatite complexes related to nepheline syenites (Bagdasarov 1990).

The REE contents in Carbonatites I of the IVAC (700–1,600 ppm) correspond to those in high-temperature carbonatites related to ultramafic-alkaline complexes. In Carbonatites II, total REE increases up to 3,210 ppm. The highest ∑REE contents (7,480–48,000 ppm) were determined in

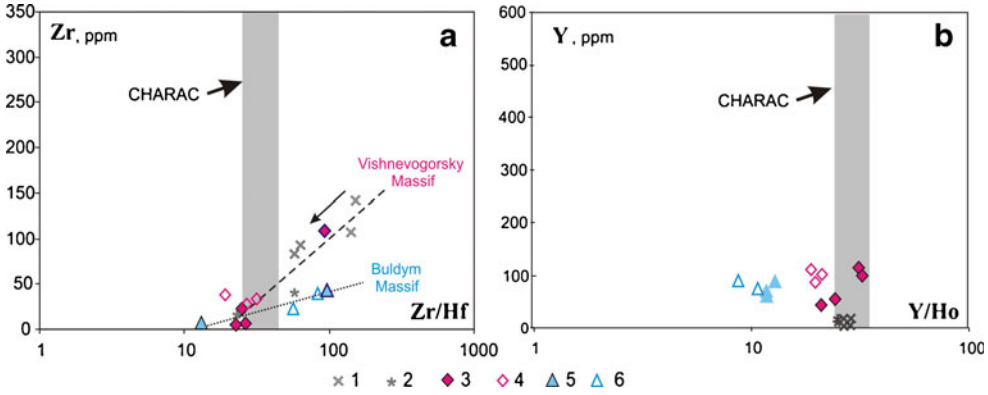

Fig. 5 Zr vs. Zr/Hf (**a**) and Y vs. Y/Ho (**b**) diagrams for carbonatites and miaskites of IVAC in respect to CHARAC field (Bau 1996). *1* – Miaskite, Vishnevogorsky Massif; *2* – Miaskite, Central Alkaline Belt; *3* – Sövite I, *4* – Sövite II; *5* – Sövite III; 6 – Beforsite IV

dolomite Carbonatite IV from the Buldym Massif. This carbonatite contains monazite, aeschynite, and allanite; the total REE and LREE contents increase from the early carbonatites to the late ones. The Eu/Eu* ratios in the early carbonatites of the IVAC are close to unity as in miaskite, confirming the idea of carbonatite liquid fractionated from a miaskitic magma. The Eu/Eu* ratios in carbonatites systematically decrease from the early to the late generations, i.e. from 0.95 to 0.60, indicating accumulation of Eu in early carbonatites, as is commonly noted in all fractionated carbonatite complexes.

The Y/Ho ratios of the early Carbonatites I (24–32), and miaskites of the IVAC as well, are close to chondrite values (Fig. 5b), showing CHARAC-behavior of the Y and Ho during carbonatite melt formation. For the late Carbonatites II Y/Ho ratios are far away from the CHARAC field, typical for the fluid-hydrothermal carbonate systems (Bau 1996).

Thus, from the early to the late carbonatites of the IVAC, Sr, Nb, and REE are gained (note that the REE enrichment has two maxima – during Sövite II formation and prior to the Buldym Massif formation); the LREE/HREE ratio increases; the Ba/Sr, Zr/Hf and Eu/Eu* ratios decrease; the Nb/Ta ratio increases. In general, these trends correspond to the evolution of carbonatitic magmas in ultramafic-alkaline complexes (Samoilov 1984).

The principal compositional difference of the IVAC carbonatites compared to those from ultramafic-alkaline complexes consists in higher Sr contents in the early carbonatites and, as a result, the absence of significant concentrations of this element and a lack of Sr minerals in the late low-temperature carbonatites. Ba, Nb, Ta, Ti, Zr, and Hf concentrations are also low, and HREE contents are somewhat higher, consequently La/Yb ratios decrease (Table 1, Figs. 3, 4 and 5). These features are noted for carbonatite complexes related with nepheline syenites and linear zones of alkaline metasomatites; i.e. the so-called "carbonatites of the linear fracture zones" (Borodin 1966; 1994; Ginzburg and Samoilov 1983; Bagdasarov 1990) or "meta-carbonatite complexes" where the rocks show the features of hydrothermal reworking and substance replacements. Furthermore, these features underline the specific nature of the IVAC carbonatites, evidently related to fractionation of miaskitic magma, contrasting with carbonatites from ultramafic-alkaline complexes that formed by fractionation of parental ultramafic-alkaline melts.

PT conditions of the IVAC rock formation

The crystallization temperature and pressure of the IVAC miaskites, including their contact facies, were estimated by Levin (1974) and Ronenson (1966) using two-feldspar, nepheline-feldspar, and amphibole-plagioclase geothermometers, the homogenization of fluid inclusions in nepheline, and experimental data on nepheline-feldspar eutectics. According to their results miaskites of the IVAC were crystallized at T=700–850 °C and P=2–5 kbar. A temperature of 900 °C was established in contact aureoles of miaskitic plutons from the amphibole-garnet geothermometer applied to fenitized amphibolites. The separation of immiscible silicate and carbonate melts occurred at T=1,000 °C and P= 5 kbar (Nedosekova 2007b; Nedosekova et al. 2009). According to Simonov (1981) miaskite-pegmatites were crystallized at T=590–750 °C and P=2.5–3.5 kbar.

To estimate the carbonatite and fenite formation temperatures, the biotite-pyroxene and amphibole-pyroxene geothermometers, based on partitioning of femic components between these phases (Samoilov 1977) as well as the geothermometer, based on partitioning of fluorine between coexisting biotite and apatite, and taking into account an annite-siderophyllite component (Sallet 2000), were applied. In addition, the pyrite-pyrrhotite geothermometer (Toulmin and Barton 1964), dolomite-calcite thermobarometer (Talantsev and Petrova 1991), and the improved Buddington-Lindsley titanomagnetite-ilmenite geothermometer (Poltavets 1975) were used. Chemical analyses of coexisting biotite, pyroxene, amphibole, apatite, dolomite, and calcite (Levin et al. 1997) were used for the calculations and several geothermometers were applied on the same sample. Biotite-pyroxene and amphibole-pyroxene thermometers, applied to samples from the Central Alkaline

Belt, reveal formation temperatures for melanocratic carbonate-silicate metasomatic rocks and Carbonatites II in the range of 650 to 600 °C and 590–490 °C, respectively. Both thermometers applied gave consistent temperature estimates.

The formation temperatures of Carbonatites I and II from the Central Alkaline Belt are 730–770 °C and 640–770 °C, respectively (apatite-biotite thermometer), and for carbonatites I from the Vishnevogorsky Massif (Zone 147) – 760–900 °C (apatite-biotite thermometer). Zircon crystallization temperatures for the early carbonatites of the Vishnevogorsky Massif, based on the "Ti-in" geothermometer (Watson et al. 2006), are about 670–770°C, and for carbonatites of the Buldym Massif – 580–650°C. Dolomite-calcite Carbonatites III from the Buldym Massif were formed at 410–575 °C, and dolomite carbonatites IV at 230–315 °C, according to the dolomite-calcite geothermometer (Talantsev and Petrova 1991). Sulfides in Carbonatites III were formed at the final stages at 330–350 °C, based on the pyrite pyrrhotite thermometry.

IVAC isotope geochronology

The first Rb-Sr and U-Pb isotope data for the rocks of the IVAC were obtained in the 70ies and 80ies of the 20th century (Kononova et al. 1979; Kramm et al. 1983, 1993; Chernyshev et al. 1987). Whole-rock Rb-Sr isochrones for the miaskites of the IVAC yielded ages of 446±12 Ma (Ilmenogorsky Massif; Kramm et al. 1983) and 436±31 Ma (Vishnevogorsky Massif; Kononova et al. 1979). These ages were interpreted as intrusion ages of the miaskite plutons during the final stage of the continental rifting at the Ordovician to Silurian boundary. However, Rb-Sr mineral isochrones revealed ages of 245±8 Ma (Kononova et al. 1979) and 245±24 Ma (Kramm et al. 1983) for the miaskites. These younger ages were related to a metamorphic overprint during which new isotopic equilibria between the minerals were established.

The TIMS U-Pb ages for one group of zircons (Zircon I) from IVAC is 434±15 Ma (Kramm et al. 1993), 422±10 Ma for miaskite and 432±12 Ma for carbonatites (Chernyshev et al. 1987). Thus, TIMS U-Pb zircon dating demonstrates the same chronology for the geological events in the evolution of the carbonatites and miaskites. U-Pb zircon systems as well as Rb-Sr reflect metamorphic overprinting events, which are accompanied by the radiogenic Pb loss and gave 261±14 Ma for miaskites and 261±12 Ma for carbonatites (Chernyshev et al. 1987).

In this study we have investigated zircons from miaskites and carbonatites of the Vishnevogorsky Massif as well as from dolomitic carbonatites of the Buldym Massif by the "in-situ" isotope methods (SHRIMP II and LA-ICP MS). Additionally, U-Pb isotopic ages of the pyrochlores from the miaskite-pegmatite of the Vishnevogorsky Massif and dolomite-calcite carbonatites of the Buldym Massif were obtained for the first time by TIMS (VSEGEI, St.-Petersburg).

SHRIMP U-Pb age of Zircon I formation (IVAC) corresponds to 417±7 Ma for miaskites (Krasnobaev et al. 2010a, b) and 411±14 Ma for carbonatites (Table 2). Alongside with it, later processes are dated by zircons of the IVAC. Most of zircon grains from miaskites and carbonatites are characterized by intermediate types and are dated at 383±14 Ma and 359±25 Ma, respectively (Krasnobaev et al. 2009, 2010a, b). U-Pb dating of the late newly formed Zircon II from miaskites and carbonatites yielded agey of 279±10 Ma (SHRIMP II) and 282 Ma (LA-ICP MS) (Table 2). The U-Pb age for zircon from dolomitic carbonatites of the Buldym Massif is 268±6 Ma and MSWD (mean square of weight deviations) equals to 8.2 (n=11, La-ICP MS) (Table 2) (Nedosekova et al. 2010). The U-Pb TIMS ages of pyrochlores from the miaskite-pegmatite of the Vishnevogorsky Massif and calcite-dolomite carbonatites of the Buldym Massif correspond to 233±3.1 Ma and 210±13 Ma (Tables 3).

K-Ar ages of biotite from miaskite and carbonatite range from 226 to 256 Ma (Levin 1974; Kononova et al. 1979), reflecting a thermal event in the evolution of the miaskites and carbonatites, which is caused by total radiogenic argon loss from the minerals.

Sm-Nd and Rb-Sr isotopic systems for rocks and constituent minerals of the Vishnevogorsky and Buldym Massifs have been analyzed by HR-TIMS at IGG UD and GI KSC. A six-points whole rock Rb-Sr isochron for the miaskites and carbonatites of the Vishnevogorsky Massif corresponds to the IVAC age at 438±8 Ma and MSWD=0.62. However, the Sm-Nd system, applied to miaskites and carbonatites of the IVAC, seems to be slightly disturbed and does not give meaningful whole-rock isochrones. Alkali metasomatic processes within the ultramafic rocks of the Buldym Massif are evident at 443±23 Ma (MSWD=0.46) and 324±7 Ma (MSWD=0.64, n=5, Sm-Nd isotope data).

The isotope dating results from the IVAC, based on several isotopic systems and including whole rock, as well as mineral data, revealed several age clusters: a) 446–410 Ma (Late Ordovician-Early Devonian), b) 390–360 Ma (Middle-Late Devonian), c) 335–325 Ma (Early Carboniferous) and d) 280–230 Ma (Permian-Triassic). The corresponding events have been dated in other structural complexes of the Middle Urals (Echtler et al. 1997; Krasnobaev and Davydov 2000). The age clusters ranging from 446 Ma to 230 Ma clearly reflect the complex magmatic and geotectonic history of the IVAC, as a part of the Uralian Fold Belt, including rifting, subduction, plate collision, anatexis, and metasomatism connected with post-collisional extension.

Table 2 U-Pb isotope data of IVAC zircons

Locality	Analysis	U	Th	Pb	Isotopic ratios								D, %	Age $^{206}Pb/^{238}U$ Ma
					$^{207}Pb/^{206}Pb$	±1σ, %	$^{207}Pb/^{235}U$	±1σ, %	$^{206}Pb/^{238}U$	±1σ, %	$^{238}U/^{232}Th$	±1σ, %		
Buldym Massif	K103-02	9	77	0.20	0.0590	19	0.3507	19	0.0431	4	0.11	9	53	272±22
	K103-03	14	51	0.23	0.0716	9	0.4206	9	0.0426	3	0.28	7	74	269±14
	K103-10	37	146	0.67	0.0511	5	0.3054	5	0.0433	2	0.25	8	-11	273±8
	K103-12	27	104	0.42	0.0510	12	0.2980	12	0.0424	3	0.25	8	-11	268±16
	K103-13	11	65	0.27	0.0627	15	0.3679	14	0.0426	4	0.17	6	63	269±20
	K103-15	24	96	0.48	0.0705	8	0.4016	7	0.0414	2	0.25	8	74	261±12
	K103-16	14	59	0.21	0.0567	12	0.3287	11	0.0420	3	0.24	4	46	265±14
	K103-17	19	141	0.32	0.0589	9	0.3421	9	0.0422	2	0.13	8	54	266±12
	K103-19	10	34	0.17	0.0346	27	0.2035	26	0.0427	4	0.30	7	-143	269±20
	K103-20	27	104	0.43	0.0539	9	0.3157	8	0.0425	2	0.26	8	27	268±14
	K103-21	10	54	0.11	0.0629	27	0.3651	26	0.0421	7	0.18	6	64	266±36
Vishnevogorsky Massif	V354-2	118	13	1.04	0.0517	6	0.3190	6	0.0447	2	8.90	6	-3	282±6
	V354-3	71	147	0.52	0.0630	10	0.5770	9	0.0664	3	0.47	6	43	415±14
	V354-5	1,227	4,554	37.9	0.0543	6	0.4960	5	0.0662	2	0.27	7	-8	413±9
	V354-6	27	17	0.43	0.0543	10	0.4826	9	0.0645	3	1.61	6	-5	403±13

Table 3 U-Pb isotope data of IVAC pyrochlores

Locality	Weight, mg	U, ppm	Pb_c ppm	^{206}Pb nm/g	Isotopic ratios							Age (Ma)			Rho
					$^{206}Pb/^{204}Pb$ (meas)	$^{206*}Pb/^{238}U$	±2σ %	$^{207*}Pb/^{235}U$	±2σ %	$^{207*}Pb/^{206*}Pb$	±2σ %	$^{206*}Pb/^{238}U$	$^{207*}Pb/^{235}U$	$^{207*}Pb/^{206*}Pb$	
Vishnevogorsky Massif	0.958	965.7	48.53	182.7	55.483	0.03088	0.14	0.21901	0.51	0.05143	0.49	196.1	201.1	260.2	0.33
	3.256	1,444	47.07	277.3	87.732	0.03665	0.32	0.25696	0.38	0.05086	0.21	232.0	232.2	234.3	0.84
Buldym Massif	2.897	636.1	30.76	82.24	39.755	0.01706	0.19	0.12722	0.71	0.05409	0.66	109.0	121.6	374.9	0.37
	2.145	620.1	55.24	135.4	36.569	0.02669	0.41	0.18874	0.89	0.05128	0.76	169.8	175.6	253.6	0.52
	6.112	53.86	8.02	19.37	35.732	0.04330	0.53	0.43022	0.91	0.07207	0.74	273.2	363.3	987.8	0.59

Errors are quoted at 2-sigma level; Pbc and Pb* indicate the common and radiogenic portions, respectively. $^{206}Pb/^{204}Pb$ - measured ratio, Rho - coefficient correlation of $^{206*}Pb/^{238}U$ and $^{207*}Pb/^{235}U$ errors

Isotope geochemistry and mantle sources of the IVAC

Previous isotopic studies of the IVAC indicated a deep (mantle) source for miaskitic and carbonatitic magmas (Kononova et al. 1979). On the basis of Sr, C, and O isotopic data it was concluded that the carbonate veins of the IVAC should be classified as carbonatites. The low initial $^{87}Sr/^{86}Sr$ ratio of –0.703 and extremely homogeneous isotopic compositions of oxygen and carbon ($\delta^{18}O$ = +6.4 to +8.5‰ and average $\delta^{13}C$ = –7.3‰) throughout the 150 km alkaline belt confirm the suggested deep source of the IVAC, and no significant isotope exchange reactions with the host rocks can be assumed.

In this study we determined the $\delta^{18}O$ VSMOW and $\delta^{13}C$ VPDB isotopic compositions of calcite and dolomite from IVAC carbonatites and calciphyre (Table 4). $\delta^{18}O$ VSMOW were also obtained from phlogopite, richterite and magnetite. Initial $^{87}Sr/^{86}Sr$ and $^{143}Nd/^{144}Nd$ ratios were determined in miaskites, fenites IVAC and Buldym ultramafic rocks, as well as in calcite, dolomite, amphibole, phlogopite from IVAC carbonatites and calciphyre. Figure 6 summarizes the C and O isotopic compositions. The carbonatites of the IVAC plot into the field of primary mantle carbonatites (Yavoy and Pineau 1986; Ray and Ramesh 2000; Table 4).

The C and O isotope compositions of calcites from Sövite I and II of the Ilmenogorsky and Vishnevogorsky Massifs are identical ($\delta^{13}C$ = –6.3 to –7.0‰ and $\delta^{18}O$ = +7.6 to +7.8‰) and somewhat different from signatures, which are typical for carbonatites of the Buldym Massif and the Central Alkaline Belt. Carbonatites from the Buldym Massif, Zone 140, and Vein 125 are characterized by similar carbon and oxygen isotope composition and differ from carbonatites of the Vishnevogorsky Massif by a lighter carbon. The values of $\delta^{13}C$ of –7.4 to –8.2 ‰ and $\delta^{18}O$ +8.0 to +9.0‰ in sövite III of the Buldym Massif are slightly but systematically different from Sövite I and II of the Vishnevogorsky Massif, in agreement with Sr-Nd isotopic data. Beforsite IV from the Buldym Massif is enriched in heavy oxygen ($\delta^{18}O$ = +8.0 to +10.4‰). Carbonatites hosted in ultramafic rocks (Ilmenogorsky ore occurrence, Pit 97) are characterized by the highest $\delta^{18}O$ values (+10.7‰) and are close, in this respect, to dolomite carbonatites of the Buldym Massif.

The shift of $\delta^{18}O$ and $\delta^{13}C$ of dolomite carbonatite (Fig. 6) towards relatively elevated values compared to calico-carbonatite corresponds to the trend of Rayleigh isotope fractionation in the course of carbonatite melt crystallization with formation of a solid phase relatively depleted in these isotopes, and separation of an isotope enriched fluid phase (Ray and Ramesh 2000). Amphibole and phlogopite from carbonatites of the Buldym Massif are characterized by $\delta^{18}O$ = +5.8 and +5.4‰, correspondingly, which are close to mantle values 5.5±

Table 4 Sm-Nd-, Rb-Sr- and C-O-isotopic data of rocks and minerals of the IVAC

Rock	Mineral	Locality	Rb	Sr	$(^{87}Sr/^{86}Sr)_{440}$	ε_{Sr} 440 Ma	Sm	Nd	$^{147}Sm/^{144}Nd$	$^{143}Nd/^{144}Nd$	$(^{143}Nd/^{144}Nd)_{440}$	ε_{Nd} 440 Ma	$\delta^{13}C$, ‰ (PDB)	$\delta^{18}O$, ‰ (SMOW)
Sövite I	Calcite	Il'menogorsky Massif		9,166									-6.6	7.7
Sövite I	Calcite	Vishnevogorsky Massif		9,247	0.70356	-6.0	50.8	368	0.08510	0.512460	0.512219	2.9	-6.3	7.7
Sövite I	Calcite	Central Alkaline Belt	0.1	12,231	0.70371	-8.5	50.0	328	0.09232	0.512584	0.512318	4.8		
Sövite I	Calcite	Central Alkaline Belt											-5.6	8.0
Sövite I	Calcite	Central Alkaline Belt		7,772									-5.3	7.8
Sövite II	Calcite	Vishnevogorsky Massif		21,982	0.70359	-5.6	61.4	533	0.06959	0.512507	0.512306	4.7	-7.0	7.6
Sövite II	Apatite	Vishnevogorsky Massif			0.70352	-6.6								
Sövite II	Calcite	Zone 125		21,218	0.70470	10.2	52.5	509	0.06186	0.512076	0.511896	-3.4	-8.5	7.5
Sövite II	Calcite	Zone 140	0.1	16,718	0.70421	3.2	51.0	392	0.08001	0.512230	0.511999	-1.4	-7.7	8.1
Sövite III		Buldym Massif	0.2	12,216			42.0	314	0.08091	0.512168	0.511935	-2.7		
Sövite III	Calcite	Buldym Massif		9,723	0.70455	8.0	52.1	391	0.08048	0.512172	0.511940	-2.6	-7.8	8.0
Sövite III	Richterite	Buldym Massif		222			0.46	3	0.09476	0.512187	0.511914	-3.1		5.8
Sövite III	Dolomite	Buldym Massif		8,373	0.70455	8.0	8.10	64	0.07611	0.512166	0.511947	-2.4	-7.4	9.0
Sövite III	Calcite	Buldym Massif		10,279	0.70440	5.9	39.3	292	0.08138	0.512164	0.511929	-2.8	-8.2	8.2
Sövite III	Calcite	Il'meny, mine 97		6,758									-7.6	10.7
Beforsite IV	Dolomite	Buldym Massif		9,097	0.70447	6.9	24.5	181	0.08150	0.512292	0.512057	-0.3	-7.4	9.2
Beforsite IV	Dolomite	Buldym Massif		5,334	0.70450	7.3	12.6	93	0.08190	0.512341	0.512105	0.7	-8.2	10.4
Miaskite		Vishnevogorsky Massif	79	2,095	0.70341	-8.2	3.9	27	0.08635	0.512569	0.512320	4.9		
Miaskite		Vishnevogorsky Massif	122	1,994	0.70342	-7.9	4.8	42	0.06878	0.512549	0.512351	5.5		
Miaskite		Vishnevogorsky Massif	181	4,525	0.70336	-8.8	8.3	75	0.09310	0.512550	0.512282	4.1		
Miaskite		Central Alkaline Belt	157	2,791	0.70380	-8.5	13.7	94	0.08839	0.512511	0.512256	3.6		
Fenite		Zone 125	105	383	0.70338	-8.6	18.0	133	0.08211	0.512609	0.512372	5.9		
Metaperidotite		Buldym Massif	2.27	308.73	0.70497	12.1	0.35	2.1	0.100140	0.512310	0.512021	-0.97		
Metaolivinite		Buldym Massif	3.52	21.17	0.70763	8.9			0.162067	0.512495	0.512028	-0.87		
Metaolivinite		Buldym Massif					5.2	58	0.054602	0.512213	0.512055	-0.30		
Metaolivinite	Amphibole	Buldym Massif					7.8	29	0.163303	0.512438	0.511967	-2.03		

Table 4 (continued)

Rock	Mineral	Locality	Rb	Sr	$(^{87}Sr/^{86}Sr)_{440}$	ε_{Sr} 440Ma	Sm	Nd	$^{147}Sm/^{144}Nd$	$^{143}Nd/^{144}Nd$	$(^{143}Nd/^{144}Nd)_{440}$	ε_{Nd} 440Ma	$\delta^{13}C$, ‰ (PDB)	$\delta^{18}O$, ‰ (SMOW)
Metaolivinite	Phlogopite	Buldym Massif					0.26	1.5	0.103553	0.512296	0.511997	-1.44		
Calciphyre	Calcite	Ilmenogorsky Suite	1.0	1,201	0.70817	59.4	4.36	32	0.08291	0.511992	0.511753	-6.2	-5.9	18.3

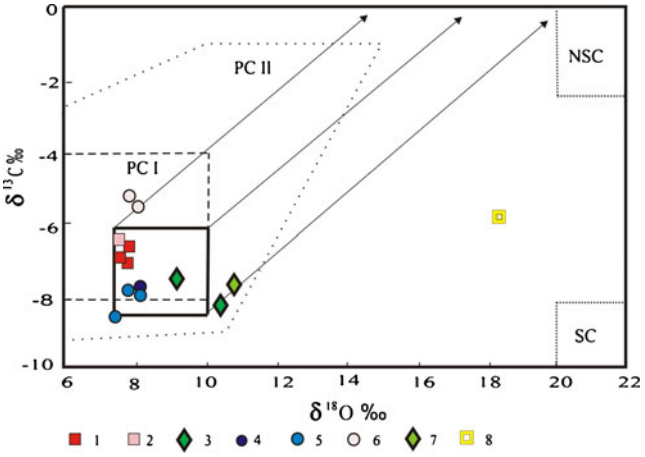

Fig. 6 Carbon and oxygen isotopic compositions of carbonates from carbonatites of the IVAC. Compositional fields: PC I – Primary carbonatites (Keller and Hoefs 1995); PC II – Primary carbonatites (Ray and Ramesh 2000); NSC – Marine sedimentary carbonates; SC – Soil carbonates (Salomons 1975). The solid bold lines are the mantle square with lines of carbonatitic magma fractionation (Yavoy and Pineau 1986). *1* – Carbonatites (sövite I, II) of the Vishnevogorsk pluton; *2* – Carbonatites of the Ilmenogorsk pluton; *3-4* – Carbonatites of the Buldym Massif: *3* – Sövite III; *4* – Beforsite IV; *5* – Carbonatites in fenites (zones 125 and 135); *6* – Carbonatites of the Central Alkaline Belt (Potanino); *7* – Carbonatites in the Ilmeny ultramafic rocks (mine 97); *8* – Calciphyres of the Ilmenogorsk Suite

0.5‰, thus they also can be considered as products of the carbonatite formation.

The carbon and oxygen isotope compositions of calcites from carbonatites of the Central Alkaline Belt (Potanino deposit) are distinguished by the highest $\delta^{13}C$ (–5.3 to –5.6‰) relatively to the early carbonatites of the Vishnevogorsky ($\delta^{13}C$ = –6.3 to –7.1‰) and Buldym ($\delta^{13}C$ = –7.4 to –8.2‰) deposits. The oxygen isotopic composition of all these carbonatites is almost identical ($\delta^{18}O$ = +7.5 to +8.2‰); the same applies to the Sr and Nd isotope compositions (Table 4). Taking into account that carbonatites of the Potaninsky and Vishnevogorsky deposits are close in chemical composition and differ only in stages of carbonatite formation, the increase in $\delta^{13}C$ may be a result of reworking of the IVAC by fluids during formation of post-collision shear zones.

Sr and Nd isotope compositions were determined from miaskites, fenites, and carbonatites of the Vishnevogorsky Massif and the Central Alkaline Belt (Potanino deposit), as well as from carbonatites and metahyperbasites of the Buldym Massif (Table 4). The initial isotope compositions of parental magmas were calculated for 440 Ma, i.e. the age of carbonatites and miaskites of the IVAC according to Kononova et al. (1979), Kramm et al. (1983, 1993), Chernyshev et al. (1987). The initial $^{87}Sr/^{86}Sr$ ratios are accepted equal to the measured values because of the low Rb/Sr ratios.

Figure 7 illustrates an εNd vs. εSr diagram of all IVAC rocks, along with mantle reservoir signatures (i.e. DM, HIMU, EMI, EM2, MORB, and OIB after Zindler and Hart 1986; Hofmann 1997). Also shown in Fig. 7 are the carbonatite isotope system evolution lines from the Kola Province (KCL, Kramm 1993) and East Africa (EACL, Bell and Petersen 1991) for comparison. The data points of carbonatites of the IVAC fit the mantle array along the line connecting depleted (DM) and enriched (EMI-like) mantle. A similar evolution line is marked for carbonatite complexes of the Kola Province, demonstrating mixing of substances from mantle reservoirs DM and EMI in the process of magma generation, in contrast to the line of the East African carbonatites, formed with a substantial contribution of the HIMU component (Bell 2001).

The initial Nd and Sr isotope ratios of the IVAC rocks are clustered in discrete fields in the εNd vs. εSr diagram (Fig. 7). Carbonatites and miaskites of the Vishnevogorsky Massif and the Central Alkaline Belt are distinguished by low $(^{87}Sr/^{86}Sr)_t$ = 0.70336–0.70380 (ε_{Sr}=–8.8 to –2.6) and the highest values of $(^{143}Nd/^{144}Nd)_t$ (ε_{Nd}=+2.9 to +4.9), corresponding to the values of moderately depleted mantle. Carbonatites of the Buldym Massif and carbonatites of Zone 125 and Zone 140 make up a cluster with higher $(^{87}Sr/^{86}Sr)_t$=0.70421–0.70470 (ε_{Sr}=+3.2 to +10.2) and low $(^{143}Nd/^{144}Nd)_t$ (ε_{Nd}=−1.4 to −3.4), corresponding to the enriched mantle EM1. Dolomite carbonatites IV from the Buldym Massif differ somewhat in $(^{143}Nd/^{144}Nd)_t$ from dolomite-calcite carbonatites III, having an identical

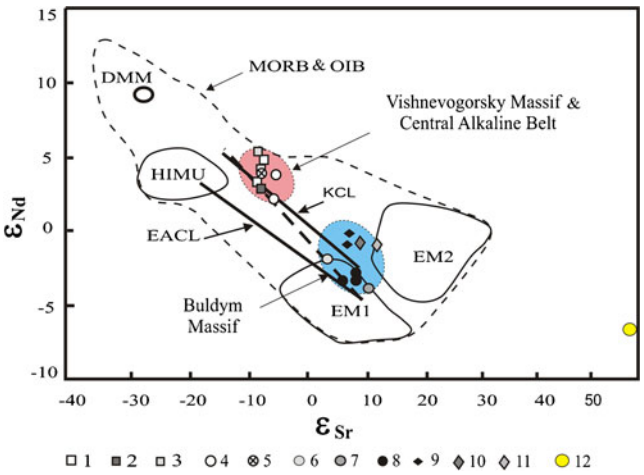

Fig. 7 Diagram of εSr vs. εNd of carbonatites, miaskites and fenites of the IVAC in respect to the Kola (KCL) and East African (EACL) carbonatites (Bell and Petersen 1991; Kramm 1993) and various mantle sources DMM, HIMU, EM1, EM2, as well as MORB and OIB (Hofmann 1997). *1-2* – Miaskites: *1* – Vishnevogorsk pluton; *2* – Central Alkaline Belt; *3* – Fenites, Zone 125; *4-5* – Sövites I: *4*– Vishnevogorsk pluton; *5* – Central Alkaline Belt; *6-7* – Sövites II: *6* – Zone 140; *7* – Zone 125; *8-11* – Rocks of the Buldym Massif: *8* – Sövites III: *9* – Beforsite IV; *10* – Metaolivinite; *11* – Metaperidotite; *12* – Calciphyres of the Ilmenogorsk Suite

$^{87}Sr/^{86}Sr$ ratio, and are similar to metahyperbasites of the Buldym Massif according the isotope signatures. The difference in isotopic signatures of carbonatites from the Vishnevogorsky and Buldym Massifs may be related to either progressive evolution of mantle isotope systems or contamination of silicate and carbonatite melts during evolution of fluid-melt systems of the IVAC.

The similarity of the Sr and Nd isotope compositions of carbonatites and miaskites of the Central Alkaline Belt and the Vishnevogorsky Massif indicate a common source. The Sr and Nd isotope signatures of carbonatites from the Central Alkaline Belt show the most depleted values (ε_{Nd}=4.8, ε_{Sr}=–8.5), close to those of miaskites, thus confirming their plausible formation at the initial stage of the development of the IVAC (Levin et al. 1997) and by fractionation from miaskite magmas.

The separate clusters of data points of carbonatites related to the IVAC plotted on the ε_{Nd} – ε_{Sr} diagram testify the multistage formation of carbonatites. Carbonatites and miaskites of the Vishnevogorsky Massif and the Central Alkaline Belt are related to a moderately depleted mantle source, while carbonatites of the Buldym Massif and zones 140 and 125 correspond to a more enriched source of EMI type. Carbonatites of the Buldym Massif probably had another source enriched in radiogenic Sr and unradiogenic Nd, which could have been related to mantle pluming, or melting of lower crust (Hofmann 1997); however, crustal contamination during the carbonatite fluid-melt evolution of the IVAC cannot be ruled out as well.

Lu-Hf- and U-Pb isotope data of zircons from miaskite, miaskitic pegmatite, and carbonatite of the Vishnevogorsky miaskitic Massif, as well as zircons of dolomitic carbonatite of the Buldym ultrabasic Massif were obtained (Table 5). Zircon of the miaskites and carbonatites of Vishnevogorsky Massif is represented by grains of several morphological types with ill-defined forms, prismatic and dipyramidal-shape, different in colour, transparency and also presence of inclusions. The early Zircon I, possibly formed during crystallization of the miaskite melt, has an irregular form. It is not transparent enough, usually darker in CL images and shows spotty BSE images with relics of growth zoning. Late Zircon II forms short-prismatic grains, is transparent, with relics of the primary zoning, highly homogeneous in BSE and with distinct CL images. However, the majority of the zircon grains is represented by an intermediate type, characterized by early zircon alteration and its replacement by a late zircon generation.

The initial ratios of Hf isotopes for the early zircon were measured on the same grains that were used for the U–Pb dating, and they demonstrate insignificant variations of $(^{176}Hf/^{177}Hf)_{410}$=0.282617–0.282678, εHf=3.5–5.7 and provide evidence for zircon formation from a moderately depleted source (Fig. 8). Zircons from

Table 5 Lu–Hf isotopic data of zircons from the IVAC rocks

Rock and Massif	Sample	$^{176}Lu/^{177}Hf$	$^{176}Yb/^{177}Hf$	$^{176}Hf/^{177}Hf$	Age $^{206}Pb/^{238}U$ (Ma)	$^{176}Hf/^{177}Hf$ (T)	εHf (T)	T_{DM} (Ga)	T_{DMC} (Ga)
Miaskite, Vishnevogorsky Massif	Vnp-2	0.00003	0.00114	0.282623	411	0.282623	+3.8	0.87	1.17
	Vnp-1A	0.00004	0.00163	0.282633	411	0.282633	+4.1	0.86	1.15
	Vnp-1B	0.00003	0.00132	0.282668	411	0.282668	+5.4	0.81	1.07
Miaskite-pegmatite, Vishnevogorsky Massif	Krv-5-1*	0.00005	0.00160	0.282617	411*	0.282617	+3.5	0.88	1.17
	Krv-5-2*	0.00004	0.00138	0.282632	411*	0.282632	+4.1	0.86	1.15
	Krv-5-3*	0.00004	0.00162	0.282654	411*	0.282654	+4.8	0.83	1.10
Sövite I, Vishnevogorsky Massif	V -3	0.00020	0.00968	0.282680	411	0.282678	+5.7	0.79	1.04
	V -6	0.00027	0.01302	0.282660	411	0.282658	+5.0	0.82	1.09
	V-8*	0.00203	0.08847	0.282679	411*	0.282663	+5.2	0.84	1.08
	V-10*	0.00006	0.00255	0.282673	411*	0.282673	+5.5	0.80	1.06
	V-12*	0.00031	0.01415	0.282664	411*	0.282662	+5.1	0.82	1.08
	V -2	0.00006	0.00235	0.283055	282	0.283055	+16.2	0.27	0.27
Beforsite IV, Buldym Massif	K103-02	0.00049	0.02142	0.282593	268	0.282591	-0.5	0.92	1.33
	K103-03	0.00025	0.01044	0.282587	268	0.282586	-0.7	0.92	1.34
	K103-10	0.00028	0.01184	0.282589	268	0.282588	-0.6	0.92	1.34
	K103-12	0.00044	0.01781	0.282601	268	0.282599	-0.2	0.91	1.31
	K103-13	0.00037	0.01598	0.282589	268	0.282587	-0.7	0.92	1.34
	K103-15	0.00035	0.01422	0.282557	268	0.282555	-1.8	0.97	1.41

Error values for the $^{176}Hf/^{177}Hf$ ratio are ±0.00002 (2σ), which is equal to ±0.7 εHf based on 91,500 zircon standard. Isotopic characteristics for chondrite after (Scherer et al. 2001) were accepted for calculations of initial Hf isotopic ratios and εHf. Asterisks denote points at which the $^{206}Pb/^{238}U$ age was not determined but was extrapolated for the calculation of the initial $^{176}Hf/^{177}Hf$ ratios and εHf (T)

miaskite, miaskitic pegmatite, and carbonatite have close Hf isotopic parameters that point to the same magmatic source (at least for Hf).

The Hf isotope composition was also analyzed on Zircon II crystals (U-Pb age of 282 Ma) from carbonatite of the Vishnevogorsky Massif. Zircon II differs significantly from

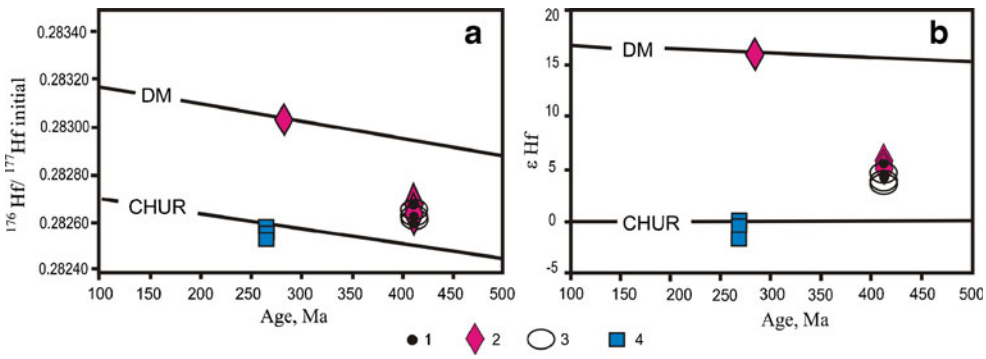

Fig. 8 Initial $^{176}Hf/^{177}Hf$ isotopic ratios and εHf in zircons from the IVAC rocks. 1-3 - Vishnevogorsky Massif: *1* – Miaskite; *2* – Carbonatite; *3* – Miaskite-pegmatite; *4* – Beforsite IV, Buldym Massif. Lines for the DM and CHUR mantle reservoirs isotopic evolution are shown for comparison. A decay constant of ^{176}Lu $\lambda=1.865\cdot10^{-11}$ is applied for the calculation of DM and CHUR isotopic evolution (Scherer et al. 2001)

early Zircon I. It has high values of $(^{176}Hf/^{177}Hf)_{282}$= 0.283055 and εHf=16, corresponding to those typical for depleted mantle that may provide evidence for the different, juvenile source of the matter participating in miaskite and carbonatite transformations. However, at present this suggestion is speculative and would need further study.

The isotope composition of Hf of zircons from dolomitic carbonatite of the Buldym Massif $(^{176}Hf/^{177}Hf)_{268}$= 0.282525–0.282555, εHf=–0.2 to –1.8 is close to that of chondrite and differs significantly from those of Vishnevogorsky Massif zircons by lower initial Hf isotope ratios and εHf. This indicates contribution of substances from various sources. Figure 9 is an εNd vs. εHf plot, where it becomes obvious that early zircon compositions of the IVAC plot in the field of moderately depleted mantle and lower crust rocks. Only one point (V-354-2, late Zircon II with age of 282 Ma from carbonatite of the Vishnevogorsky Massif) is outside the "terrestrial array" (Fig. 9; Vervoort et al. 2000), which is possibly connected with the metamorphic genesis of the Zircon II.

The origin and source of the carbonatite parental melts remains a poorly resolved problem up to now. Several sources have been suggested for carbonatites. These include the sub-lithospheric source, associated with deep-seated, plume-related activity (Gerlach et al. 1988; Simonetti et al. 1995, 1998; Bell and Simonetti 1996, 2010; Marty et al. 1998; Dunworth and Bell 2001; Bell 2001; Bell and Tilton 2001, 2002; Tolstikhin et al. 2002; Bell and Rukhlov 2004; Kogarko 2006), or either asthenospheric 'upwellings' (Bailey 1993; Bailey and Woolley 2005); subducted lithosphere (Barker 1996); lithospheric source (Bell et al. 1982; Burke and Khan 2006) and mixing between lithospheric and sub-lithospheric sources (Gerlach et al. 1988; Simonetti et al. 1998).

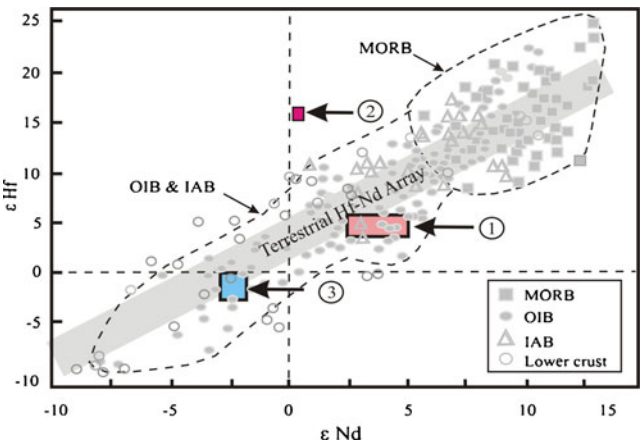

Fig. 9 εHf vs. εNd diagram of zircons from the IVAC rocks. Composition fields of zircon from: *1* – Miaskite, miaskitic pegmatite, and carbonatite of the Vishnevogorsky Massif (U-Pb ages – 410); *2* – Carbonatite of the Vishnevogorsky Massif (U-Pb ages – 282 Ma); *3* – Beforsite IV, Buldym Massif (U–Pb age – 268 Ma). Isotopic compositions of MORB, OIB and IAB (Patchett and Tastumoto 1980; Salters and White 1998, and others) and lower crustal rocks (Vervoort et al. 2000) are shown for comparison

Our new isotope data of rocks and minerals from the IVAC miaskite and carbonatites, i.e. εSr between –6 and –10, εNd between +3 and +6 and εHf between +4 and +6, require a depleted mantle source with continuous low Rb/Sr, high Lu/Hf and Sm/Nd ratios over a long period of time. This implies that the IVAC miaskite-carbonatite is fairly homogeneous in respect to all three isotopes systems studied. The initial isotope ratios plot, together with the bulk rocks, into the moderately depleted mantle field in Figs 7 and 9. A close resemblance exists between the isotope characteristics of the IVAC and carbonatites of ultramafic-alkaline carbonatite complexes (Kola Alkaline Province–Kovdor, Sockly, Lovozero, Khibina, and the Maymecha-Kotuy Alkaline Province, Polar Siberia: Guli, Essey, Ingily, and intrusions of the Northern America), which are located within Precambrian cratons (Bell and Blenkinsop 1989; Kramm 1993; Kramm and Kogarko 1994; Zaitsev and Bell 1995; Dunworth and Bell 2001; Kogarko et al. 2010). This suggests that the origin of these alkaline-ultrabasic complexes and carbonatites is connected with deep seated mantle sources, possibly related to an upwelling mantle plume (FOZO) and/or further mixing with a plume enriched with an EM1 component (Bell and Blenkinsop 1989; Kramm 1993; Bell 1998; Dunworth and Bell 2001). The hypothetical FOZO deep mantle source, suggested to be common to all plumes, has εNd around +5, according to Hart et al. (1992), which is close to the characteristics of the IVAC. Therefore, it is very likely that the IVAC has a similar source. However, the origin of the alkaline magmas of the IVAC by melting of oceanic crust (Levin et al. 1997), which has the same isotopic characteristics (Echtler et al. 1997), cannot be excluded. It should also be noted, that a decoupling of the Nd and Hf isotope compositions, shown in the late zircons of the Vishnevogorsky carbonatite, could be related to the metamorphic stage of the IVAC formation.

Sr, Nd and Hf isotope data of the carbonatites of the Buldym Massif, i.e. εSr between +6 and +8, εNd between +1 and -3, and εHf between 0 and –2, require continuous higher Rb/Sr ratio, lower Lu/Hf and Sm/Nd over a long period of time in their source (EM1-like). Demonstrated differences in Sr, Nd and Hf isotope compositions between rocks of miaskite-carbonatite complex and carbonatites of the Buldym Massif could be explained either by variable degrees of mixing a plume with an enriched mantle component, i.e. like EM1, or crustal contamination processes driven by the IVAC carbonatite fluid-melt evolution.

Silicate-carbonate liquid immiscibility and fluid-hydrothermal processes during carbonatite formation within the IVAC: evidence from trace elements and isotope data

The similarity of initial Nd and Sr isotope ratios of carbonatites and miaskites of the IVAC strongly indicates a

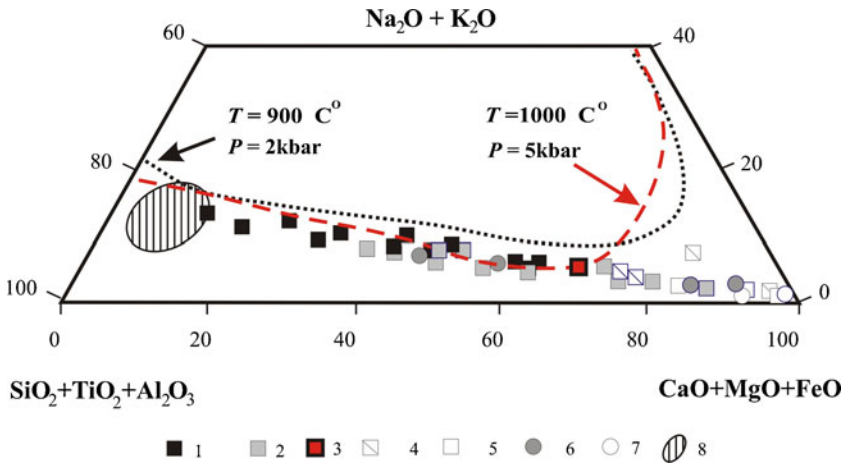

Fig. 10 Chemical compositions of the IVAC rocks plotted on the (SiO_2 + $A1_2O_3$ + TiO_2)-(CaO + MgO + FeO)-(Na_2O + K_2O) diagram (Freestone and Hamilton 1980). *1* – Melanocratic carbonate-silicate rock; *2* – Sövite I; *3* – Brechia Dyke of carbonatites *4* – Sövite II (Vishnevogorsky Massif, zone 147); *5* – Sövite II (Potanino); *6* – Sövite III (Buldym Massif); *7* – Beforsite IV (Buldym Massif); *8* – Miaskite of the Vishnevogorsky pluton and Central Alkaline Belt. The dashed line is the miscibility gap between carbonate and silicate melts at T=1,000 °C and P=5 kbar; the dotted line is the same gap at T= 900 °C and P=2 kbar (Kjarsgaard 1998)

common source. This raises the question whether partition of a parental carbonated miaskitic melt into a silicate and a carbonate liquid has taken place. Evidences for such a process derive from geological observations, trace element patterns, isotope data (i.e. Fig. 7; Nedosekova 2007b) and the occurrence of salt melt inclusions in miaskites of the IVAC (Simonov 1981; Talantsev and Petrova 1991).

Support for the suggested possibility of immiscibility into silicate and carbonate liquids evolves from Fig. 10, a Freestone-Hamilton diagram (Kjarsgaard and Hamilton 1989). The IVAC carbonatites, based on major element composition, plot right onto the line of immiscibility constrained at a temperature of 1,000 °C and at 5 kbar pressure. Additional support for immiscibility derives from trace elements and REE. Trace element partition coefficients (D) calculated, based on miaskite samples and their Y/Ho and Zr/Hf ratios, from early and late carbonatites are different. D values calculated from Carbonatites I and miaskites of the Vishnevogorsky Massif are: Sr (4.5–6), Ba (0.44–1.92), Zr (0.01–0.33), Hf (0.03–0.24), Nb (0.5–0.8), Ta (0.09–0.43). These D values are similar to those experimentally determined by Hamilton et al. (1989), Veksler et al. (1998) for

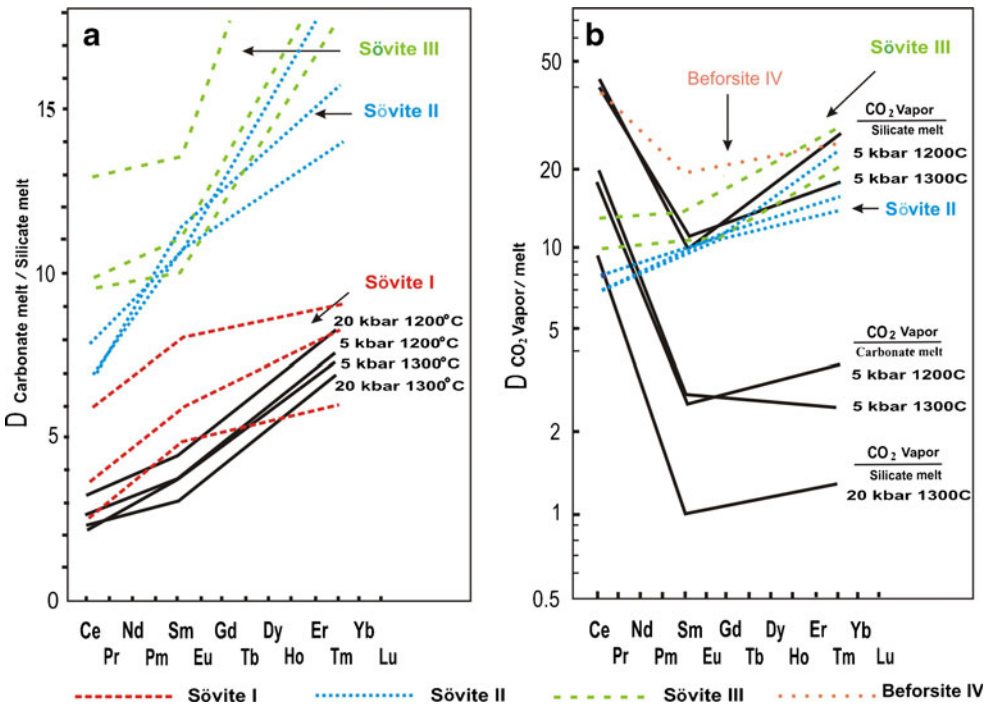

Fig. 11 Partitioning coefficients of REE (D_{REE}) between the IVAC Carbonatites I and miaskite (*dashed lines* I - red) and between the late carbonatites (II, III, IV) and miaskite (*dotted lines* II - blue, III - green, IV - brown). The experimentally determined D_{REE} (*solid lines*) are shown for comparison: (**a**) between coexisting carbonate and silicate melts at T= 1,200-1,300 °C and P=5-20 kbar; (**b**) between coexisting CO_2 vapor and silicate melt at T= 1,200-1,300 °C and P=5 kbar; between CO_2 vapor and carbonate melt at T=1,200-1,300 °C and P=5 kbar; between CO_2 vapor and silicate melt at T=1,300 °C and P=20 kbar (Wendlandt and Harrison 1979)

silicate-carbonate liquid immiscibility in alkaline melts at P=0.8–1 kbar T=965–1,150 °C (Fig. 12). REE partition coefficients calculated from IVAC Carbonatites I and miaskites, i.e. Ce (3–7), Sm (5–8), Tb (6–9), are higher than those obtained from experiments, stated above, and correspond to D values for silicate-carbonate liquid immiscibility at P=5 kbar and T=1200 °C (Fig. 11a; Wendlandt and Harrison 1979). Carbonatites II and III show higher D values, i.e. Ce (10–38), Sm (11–18), Tb (14–28), close to values between carbonate fluid and silicate melt (Wendlandt and Harrison 1979). This clearly indicates the significant role of an alkali carbonate fluid in the formation of late carbonatites of the IVAC (Fig. 11b).

Conclusions

The Ilmeny-Vishnevogorsky alkaline complex intruded into the crystalline basement (Paleoproterozoic) at the Ordovician/Silurian boundary and underwent significant reworking during Ural Fold Belt formation. The present geochronological data of the IVAC mirror clearly the magmatic intrusion of alkaline rocks and carbonatites (Late Ordovician) and a long-lasting metamorphic overprint, involving anatexis, pegmatite formation, metasomatism and ore deposit formation, attributed to the rift-related (Silurian-Early Devonian), collision (Middle-Late Devonian, Early Carboniferous) and post-collision (Permian-Triassic) stages during the evolution of the Ural Belt.

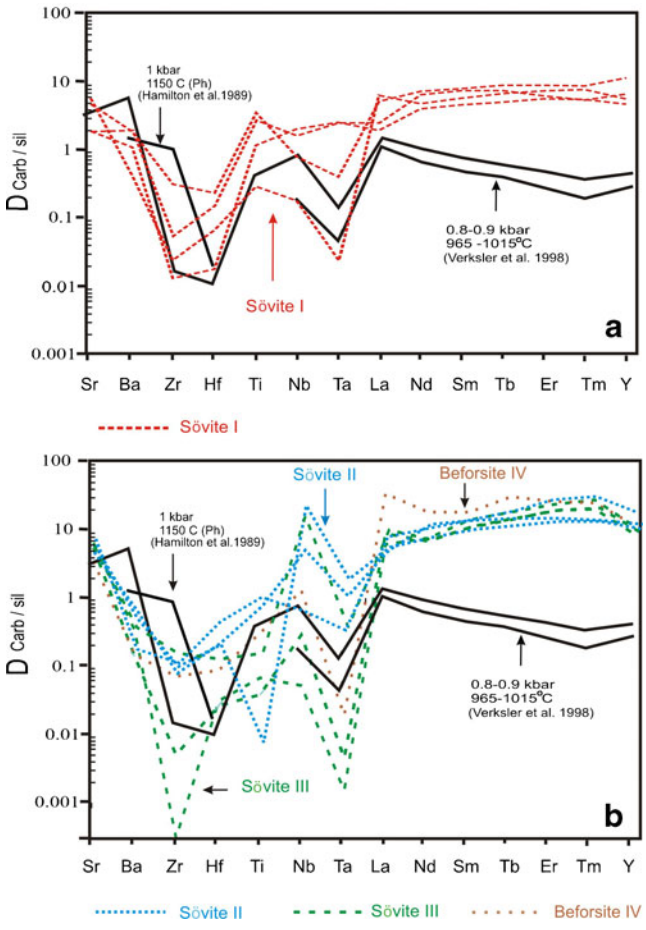

Fig. 12 Carbonate-silicate partitioning coefficients for trace elements in the IVAC rocks, in comparison to experimental data at T=965-1,150 °C and P=0.8-1 kbar (Hamilton et al. 1989; Veksler et al. 1998). Ph – phonolite-alkali carbonatites system. A) *dashed red line* – Sövite I - miaskite; B) *dotted blue lines* – Sövite II - miaskite

The IVAC was formed at T=1,000-230 °C and P=5-2 kbar. Immiscibility of an initial carbonated miaskite melt occurred at T=1,000 °C and P=5 kbar. Miaskite crystallized at T=850-700 °C and P=2-5 kbar, whereas miaskite-pegmatites at T=750-590°C and P=2.5–3.5 kbar. The formation temperature (700–900 °C) of early carbonatites (Sövite I) and fenites is close to the temperature of crystallization of miaskites. Sövite I and melanocratic carbonate-silicate rocks of the Central Alkaline Belt were formed at 600–650 °C and Sövite II at 500–600 °C. Dolomite-calcite sövite III and Beforsite IV from the Buldym Massif crystallized at T=575-410 °C and T=315-230 °C, respectively.

Geological, geochemical and isotopic data indicate a possible separation of cabronatite liquid from miaskitic magma. It is most likely that silicate-carbonate liquid immiscibility, regarding the formation of early carbonatites and miaskites, took place. IVAC rock compositions correspond to the boundary of silicate and carbonate melts, experimentally determined at T=1,000 °C and P=5 kbar. REE partition coefficients between early IVAC carbonatite and miaskite match with those of an initial alkaline melt at immiscibility into silicate and carbonate liquids at the same P-T-conditions mentioned above. Isotope data from carbonatites and miaskites also indicate the separation of a carbonatite liquid from a miaskitic silicate magma. Trace element data from late stage IVAC carbonatites indicate the significant role of an alkali-carbonate fluid.

The geochemical evolution of the IVAC carbonatites show similarities to that of ultramafic-alkaline complexes and related carbonatites. This is indicated by: (1) elevated concentrations of Sr, Ba, Nb, and REE with two maxima of REE and Sr, one at the albite-calcite and the second at the chlorite-sericite-ankerite facies; (2) an increase in the LREE/HREE ratio with decreasing crystallization temperature; and (3) systematic variations in Sr/Ba, Nb/Ta, Zr/Hf, La/Yb, and Eu/Eu* ratios from the early to late members of carbonatite series due to the evolution of carbonatitic melt and its fluid derivatives.

Carbonatites of the IVAC differ in geochemical features from carbonatites of the ultramafic-alkaline complexes and have much in common with carbonatites related to nepheline syenites and carbonatites localized in linear fracture zones. This is manifested in the high Sr contents in early carbonatites

and, as a consequence, the absence of significant Sr concentrations and Sr minerals in late, low-temperature carbonatites; a slight depletion in Ba, Nb, Ta, Ti, Zr, and Hf; and enrichment in HREE, marked by a decreased La/Yb ratio, relative to carbonatites of ultramafic-alkaline complexes.

Sr, Nd, C, O, and Hf isotope data suggest a mantle source of the IVAC and indicate that material of a moderately depleted mantle (DM) and an EMI-type enriched component participated in magma generation. The significant difference in the carbonatite isotopic data from the Vishnevogorsky pluton and the Buldym Massif clearly testifies their different sources and the multistage formation of the IVAC carbonatites. Carbonatites and miaskites of the Vishnevogorsky Massif have a moderately depleted mantle source. Carbonatites of the Buldym Massif were derived from an enriched source. Contamination cannot be excluded in the formation of these carbonatites, e.g. based on isotopic evidence, the lower crust could have participated in the generation of magma that produced the IVAC. The strong differences in the isotopic signature of the carbonatites from Vishnevogorsky and Buldym Massifs could be explained by different extent of the mixing of the plume component and enriched component (EM_1 like), or by processes of crustal contamination during evolution of the IVAC carbonatite fluid-melts.

Consequently, the origin and genesis of Ilmeny-Vishnevogorsky carbonatite-miaskite complex is related to mantle anatexis and subsequent mantle-crust interaction. As a result, fluid-saturated miaskite and carbonatite were formed. The isotopic and geochemical data of this study shows that the carbonatites of the IVAC are genetically related to miaskites and are distinct from carbonatites derived from ultramafic-alkaline melts.

Acknowledgments We thank LN Kogarko, NV Vladykin, VYa Levin, and VN Sazonov for consultations and fruitful discussions. The authors are highly indebted to staff of the analytical lab and YL Ronkin at the IGG for carrying out isotope and geochemical analyses. This study was carried out as a part of integration projects of the Ural Branch, Siberian Division, and Far East Division of the Russian Academy of Sciences № 12-C-5-103 and by program № 12-P-5-2015. We express our sincere thanks to guest editor OAR Thalhammer for handling this manuscript and for his editorial input.

References

Bagdasarov YA (1979) Linear fracture bodies of carbonatites: a new subdivision of alkaline ultramafic-carbonatite complexes. Dokl Akad Nauk SSSR 248:412–415 (in Russian)

Bagdasarov YA (1990) The main geochemical features of linear-type carbonatites and conditions of their formation. Geochem 28:1108–1119 (in Russian)

Bagdasarov YA (1994) Rare-metal ore potential of igneous and hydrothermal metasomatic carbonatites. Geol Ore Deposits 36:326–335

Bailey DK (1993) Carbonate magmas. J Geol Soc 150:637–651

Bailey DK, Woolley AR (2005) Repeated synchronous magmatism within Africa: timing, magnetic reversals, and global tectonics. In: Foulger GR, Natland JH, Presnall DC, Anderson DL (eds) Plates, plumes and paradigms. Geol Soc Am Spec Paper 388:365–377

Barker DS (1996) Consequences of recycled carbon in carbonatites. Can Mineral 34:373–387

Bau M (1996) Controls on the fractionation of isovalent trace elements in magmatic and aqueous systems: evidence from Y/Ho, Zr/Hf, and lantanide tetrad effect. Contrib Mineral Petrol 123:323–333

Bell K (1998) Radiogenic isotope constraints on relationships between carbonatites and associated silicate rocks—a brief review. J Petrology 39(11-12):1987–1996

Bell K (2001) Carbonatites: relationships to mantle plume activity. In: Ernst R, Buchan KL (eds) Mantle plumes: their identification through time. Geol Soc Am Spec Paper 352:267–290

Bell K, Blenkinsop J (1989) Neodymium and strontium isotope geochemistry of carbonatites. In: Bell K (ed) Carbonatites: genesis and evolution. Unwin Hyman, London, pp 278–300

Bell K, Petersen T (1991) Nd and Sr Isotope systematics of Shombole Volcano, East Africa, and the links between nephelinite, phonolites and carbonatites. Geology 19:582–585

Bell K, Rukhlov AS (2004) Carbonatites from the Kola Alkaline Province: origin, evolution and source characteristics. In: Zaitsev A, Wall F (eds) Phoscorites and carbonatites from mantle to mine: the key example of the Kola Alkaline Province. Miner Soc Series, London, pp 421–455

Bell K, Simonetti A (1996) Carbonatite magmatism and plume activity: implications from the Nd, Pb and Sr isotope systematics of Oldoinyo Lengai. J Petrol 37:1321–1339

Bell K, Simonetti A (2010) Source of parental melts to carbonatites–critical isotopic constraints. Mineral Petrol 98:77–89

Bell K, Tilton GR (2001) Nd, Pb and Sr isotopic compositions of east African carbonatites: evidence for mantle mixing and plume inhomogeneity. J Petrol 42:1927–1945

Bell K, Tilton GR (2002) Probing the mantle: the story from carbonatites. EOS Amer Geophys Union 83:276–277

Bell K, Blenkinsop J, Cole TJS, Menagh DP (1982) Evidence from Sr isotopes for long-lived heterogeneities in the upper mantle. Nature 298:251–253

Borodin LS (1966) Carbonatite deposits of the Rare Elements. In: Vlasov KA (ed) Geochemistry, mineralogy and genetic types of the Rare-Element deposits, 3rd edn. Nauka, Moscow, pp 215–256 (in Russian)

Borodin LS (1994) Genetic types and geochemistry of mantle-crustal carbonatites. Geochem 32:1683–1692 (in Russian)

Burke K, Khan S (2006) Geoinformatic approach to global nepheline syenite and carbonatites distribution: testing a Wilson cycle model. Geosphere 2:53–60

Chernyshev V, Kononova VA, Kramm U et al (1987) Isotopic geochronology of alkaline rocks of the Urals in the light of U-Pb methods on zircons. Geochem 25:323–338 (in Russian)

Dunworth E, Bell K (2001) The Turuy massif, Kola Peninsula, Russia: isotopic and geochemical evidence for multi-source evolution. J Petrol 42:377–405

Echtler HP, Ivanov KS, Ronkin YL et al (1997) The tectonometamorphic evolution of gneiss complexes in the Middle Urals, Russia. Tectonophys 276:229–251

Egorov LS (1990) Diversity of carbonatites and pseudocarbonatites. Zap Vsesoyuz Mineral Obshch 119:99–111 (in Russian)

Fabio RD, Möller P, Dulski P (2002) Zr/Hf in carbonatites and alkaline rocks: new date and a re-evaluation. Rev Brasil de Geoci 32:361–370

Freestone JC, Hamilton DL (1980) The role of liquid immiscibility in the genesis of carbonatites: an experimental study. Contrib Mineral Petrol 73:105–117

Gerlach DC, Cliff RA, Davies GR, Norry M, Hodgson N (1988) Magma sources of the Cape Verdes archipelago: isotopic and trace element constraints. Geochim Cosmochim Acta 52:2979–2992

Ginzburg AI, Samoilov VS (1983) To problems of carbonatites. Zap Vsesoyuzn Mineral Obshch 112:164–176 (In Russian)
Gittnis I, Harmer RE (1997) What is ferrocarbonatite? J Afr Earth Sci 25:159–168
Glevassky EB, Krivdik SG (1981) Precambrian carbonatite complex of the Azov region. Naukova Dumka, Kiev (in Russian)
Griffin WL, Pearson NJ, Belousova EA et al (2000) The Hf isotope composition of cratonic mantle: LAM-MC-ICPMS analysis of zircon megacrysts in kimberlites. Geochim Cosmochim Acta 64:133–147
Hamilton DL, Bedson P, Epsson J (1989) The behaviour of trace elements in the evolution of carbonatites. In: Bell K (ed) Carbonatites: genesis and evolution. Unwin Hyman, London, pp 405–427
Hart SR, Hauri E, Oschmann LA, Whitehead JA (1992) Mantle plumes and entrainment: isotopic evidence. Science 256:517–520
Hofmann AW (1997) Mantle geochemistry: the message from oceanic volcanism. Nature 385:219–229
Keller I, Hoefs I (1995) Stable isotope characteristics of recent natrocarbonatite from Oldoinyo Lengai in carbonatite volcanism: Oldoinyo Lengai and the petrogenesis of natrocarbonatites. Proceed Volcanol 4:113–236
Kjarsgaard BA (1998) Phase relations of carbonated high-CaO nephelinite at 0.2 and 0.5 Gpa. J Petrol 39:2061–2075
Kjarsgaard BA, Hamilton DL (1989) Genesis of carbonatites by liquid immiscibility. In: Bell K (ed) Carbonatites: genesis and evolution. Unwin Hyman, London, pp 388–404
Kogarko LN (2006) Enriched mantle reservoirs are the source of alkaline magmatism. In: Vladykin NV (ed) Deep-seated magmatism, its sources and plumes. Inst Geogr SB RAS, Irkutsk, pp 46–58
Kogarko LN, Lahaye Y, Brey GP (2010) Plume-related mantle source of super-large rare metal deposits from the Lovozero and Khibina massifs on the Kola Peninsula, Eastern part of Baltic shield: Sr, Nd and Hf isotope systematics. Mineral Petrol 98:197–208
Kononova VA, Dontsova EI, Kuznetsova LD (1979) Oxygen and strontium isotopic composition of the Il'mensky-Vishnevogorsky alkaline complex and genesis of miaskites. Geochem 17:1784–1795 (in Russian)
Kramm U (1993) Mantle components of carbonatite from the Kola Alkaline Province, Russia and Finland: a Nd-Sr study. Eur J Mineral 5:985–989
Kramm U, Kogarko LN (1994) Nd and Sr isotope signatures of the Khibina and Lovozero agpaitic centers, Kola alkaline province, Russia. Lithos 32:225–242
Kramm U, Blaxland AB, Kononova VA, Grauert B (1983) Origin of the Ilmenogorsk-Vishnevogorsk nepheline syenites, Urals, USSR, and their time of emplacement during the history of the Ural Fold Belt: a Rb-Sr study. J Geol 91:427–435
Kramm U, Chernyshev IV, Grauert S et al (1993) Zircon typology and U-Pb systematics: a case study of zircons from nepheline syenite of the Il'meny Mountains, Ural. Petrology 1:474–485
Krasnobaev AA, Nedosekova IL, Busharina SV (2009) Zirkonologija of carbonatites of Vishnevogorsky massif (S. Ural). IGG UD RAS Year-book - 2008:261–263 (in Russian)
Krasnobaev AA, Davydov VA (2000) Age and origin of the Il'menogorsky Sequence (Il'meny Mountains, the Southern Urals): evidence from zirconology. Dokl Earth Sci 372:672–677
Krasnobaev AA, Rusin AI, Busharina SV, Lepechina EN (2010a) Zirkonologija of amphibolitic miaskites of Il'menogorsky massif. Dokl Akad Nauk 430:227–231 (in Russian)
Krasnobaev AA, Rusin AI, Busharina SV, Lepehina EN, Medvedeva EV (2010b) Zirconology of amphibole nepheline Syenite of the Ilmenogorsky massif (South Urals). Dokl Earth Sci 430:76–79
Kravchenko SM, Gzamanske D, Fedorenko VA (2003) Geochemistry of carbonatites of the Tomtor Massif, Polar Siberia. Geochem 41:545–558
Kukharenko AA, Orlova MP, Bullach AG et al (1965) The Caledonian complex of ultrabasic, alkaline rocks and carbonatites of the Kola Peninsula and Northern Karelia. Nedra, Moscow (in Russian)
Le Bas MJ (1999) Sovite and alvikite: two chemically distinct calciocarbonatites Cl and C2. S Afr J Geol 102:109–121
Levin VY (1974) Alkaline province of the Il'meny-Vishnevye Mountains (nepheline syenites of the Urals). Nauka, Moscow (in Russian)
Levin VY, Ronenson BM, Samkov VS et al (1997) Alkaline-carbonatite complexes of the Urals. Uralgeolkom, Ekaterinburg (in Russian)
Marty B, Tolstikhin I, Kamensky IL, Nivin V, Balaganskaya E, Zimmerman JL (1998) Plume-derived rare gases in 380 Ma carbonatites from the Kola region (Russia) and the argon isotopic composition in the deep mantle. Earth Planet Sci Lett 164:179–192
Menge JN (1842) Nachricht über einen mineralogischen Ausflug in das Uralgebirge. Schr Russ Ges Min 1:105–138
Nedosekova IL (2007a) New data on carbonatites of the Il'mensky-Vishnevogorsky alkaline complex, the Southern Urals, Russia. Geol Ore Deposits 49:129–146
Nedosekova IL (2007b) Geochemical evolution and isotopic composition of carbonatites and miaskites from the Il'mensky-Vishnevogorsky complex as an indicator of silicate-carbonate immiscibility and fluid-melt interaction, the Southern Urals. In: Vladykin NV (ed) Alkaline magmatism, its sources and plumes. Inst Geogr SB RAS, Irkutsk, pp 95–123 (in Russian)
Nedosekova IL, Vladykin NV, Pribavkin SV, Bayanova TB (2009) The Il'meny-Vishnevogorsky miaskite-carbonatite complex, the Urals, Russia: origin, ore resource potential, and sources. Geol Ore Deposits 51:139–161
Nedosekova IL, Belousova EA, Sharygin VV (2010) Sources of matter for the Il'meno-Vishnevogorsky alkaline complex: evidence from Lu–Hf isotopic data for zircons. Dokl Earth Sci 435:234–239
Oktyabr'sky RA, Vrzhosek AA, Lennikov AM et al (2004) New data on carbonatites and associated rocks of the Koksharov alkaline ultramafic massif. In: VladykinI NV (ed) Deep magmatism, its sources and relationship to plume magmatism. Inst Geogr SB RAS, Irkutsk, pp 293–307 (in Russian)
Patchett PJ, Tastumoto M (1980) Hafnium isotope variations in oceanic basalts. Geophys Res Lett 7:1077–1080
Poltavets YA (1975) Discussion on the Buddington-Lindsley titanium-magnetite geothermometer on the basis of comparative analysis of equilibria between spinels of magnetite series. Izv Akad Nauk Ser Geol 6:63–72
Polyakov VO, Nedosekova IL (1990) Mineralogy of apoultramafic fenites and carbonatites in the southern Il'meny Mountains. In: Chesnokov BV (ed) Minerals of deposits and techno-genic zones in ore districts of the Urals. UD, Acad Sci USSR, Sverdlovsk, pp 24–35 (in Russian)
Rass IT, Abramov SS, Utenkov UV, Kozlovsky VM, Korpechkov DI (2006) Role of fluids in the petrogenesis of carbonatites and alkaline rocks: geochemical evidence. Geochem 44:636–655
Ray S, Ramesh R (2000) Rayleigh fractionation of stable isotopes from a multicomponent source. Geochim Cosmochim Acta 64:299–306
Ronenson BM (1966) Origin of miaskites and related rare-metal mineralization. Nedra, Moscow (in Russian)
Rose G (1839) Über die mineralogische Beschaffenheit des Ilmengebirges. Ann Phys Chem 47:373–384
Sallet R (2000) Fluorine as a tool in the petrogenesis of quartz-bearing magmatic associations: applications of an improved F-OH biotite-apatite thermometer grid. Lithos 50:241–253
Salomons W (1975) Chemical and isotopic composition of carbonatites in recent sediments and soils from Western Europe. J Sediment Petrol 45:440–449
Salters VJM, White WM (1998) Hf isotope constraints on mantle evolution. Chem Geol 145:447–460

Samoilov VS (1977) Carbonatites: fades and formation conditions. Nauka, Moscow (in Russian)
Samoilov VS (1984) Geochemistry of carbonatites. Nauka, Moscow (in Russian)
Samoilov VS, Ronenson BM (1987) Geochemistry of alkaline palingenesis. Geochem 25:1537–1546 (in Russian)
Samoilov VS, Smirnova EA (1980) Behavior of rare earth elements in carbonatite formation and some genetic aspects of carbonatites. Geochem 18:1844–1858
Scherer E, Münker C, Mezger K (2001) Calibration of the lutetium-hafnium clock. Science 293:683–687
Simonetti A, Bell K, Viladkar SG (1995) Isotopic data from the Amba Dongar carbonatite complex, west-central India: evidence for an enriched mantle source. Chem Geol 122:185–198
Simonetti A, Goldstein SL, Schmidberger SS, Viladkar SG (1998) Geochemical and Nd, Pb, and Sr isotope data from Deccan alkaline complexes-inferences for mantle sources and plumelithosphere interaction. J Petrol 39:1847–1864
Simonov VA (1981) Conditions of mineral formation in nongranitic pegmatites. Nauka, Novosibirsk (in Russian)
Sokolov SV (1991) What is carbonatite? A continued discussion. Zap Vsesoyuz Mineral Obshch 5:108–111 (in Russian)
Sun S, McDonough WF (1989) Chemical and isotopic systematics of oceanic basalts: implications for mantle composition and processes. Geol Soc 42:313–345
Talantsev AS, Petrova GA (1991) Formation conditions and mechanism of carbonatites from the Il'mensky-Vishnevogorsky alkaline complex. Nauka, Sverdlovsk (in Russian)
Tolstikhin IN, Kamensky IL, Marty B, Nivin VA, Vetrin VR, Balaganskaya EG, Ikorsky SV (2002) Rare gas isotopes and parent trace elements in ultrabasic-alkaline-carbonatite complexes, Kola Peninsula: identification of lower mantle plume component. Geochim Cosmochim Acta 66:881–901
Toulmin P, Barton PB (1964) A thermodynamic study of pyrite and pyrrhotite. Geochim Cosmochim Acta 28:651–671
Tugarinov LI, Bibikova EV, Krasnobaev AA (1970) Geochronology of uralian precambrian. Geochem 8:501–505 (in Russian)
Varlakov AS, Kuznetsdv GP, Korablev GG et al (1998) Ultramafic rocks of the Vishnevogorsky-Il'menogorsky metamorphic complex, Southern Urals. IM UB RAS, Miass (in Russian)
Veksler V, Petibon C, Jenner GA et al (1998) Trace element partitioning in immiscible silicate-carbonate liquid systems: an initial experimental study using a centrifuge autoclave. J Petrol 39:2095–2104
Vervoort JD, Patchett JP, Albarede F, Blichert-Toft J, Rudnick R, Downes H (2000) Hf-Nd isotopic evolution of the lower crust. Earth Planet Sci Lett 181:115–129
Vrublevsky VV, Pokrovsky BG, Zhuravlev DZ, Anoshin GN (2003) Composition and age of the Penchenga linear carbonatite complex, Yenisei Range. Petrol 11:130–146
Wall F, Zaitsev AN (2004) Phoscorites and carbonatites from mantle to mine: the key example of the Kola alkaline province. Mineral Soc Great Britain and Ireland, London
Watson EB, Wark DA, Thomas JB (2006) Crystallization thermometers for zircon and rutile. Contrib Mineral Petrol 151:413–433
Wendlandt RF, Harrison WJ (1979) Rare earth partitioning between immiscible carbonate and silicate liquids and CO_2 vapor. Contrib Mineral Petrol 69:409–419
Wooley AR, Kempe DRC (1989) Carbonatite: nomenclature, average chemical compositions and element distributions. In: Bell K (ed) Carbonatites: genesis and evolution. Unwin Hyman, London, pp 1–14
Yavoy M, Pineau F (1986) Carbon and nitrogen isotopes in the mantle. Chem Geol 57:41–62
Zaitsev AN, Bell K (1995) Sr and Nd isotope data of apatite, calcite and dolomite as indicators of source, and the relationships of phoscorites and carbonatites from Kovdor massif, Kola peninsula, Russia. Contrib Mineral Petrol 121:324–335
Zaraysky GP (2005) Formation conditions for rare metal deposits related to granite magmatism. In: Starostin VI (ed) Smirnov Sbornik - 2004. MGU, Moscow, pp 105–192
Zhabin AG (1959) New type of carbonatite occurrences related to the alkaline complex of the Il'meny and Vishnevye mountains on the Urals. Dokl Akad Nauk SSSR 128:1020–1022
Zindler A, Hart SR (1986) Chemical geodynamics. Ann Rev Earth Planet Sci 14:493–571
Zoloev KK, Levin VY, Mormil SI et al (2004) Minerageny and rare-metals, molybdenum, tungsten deposits of the Urals. Ministry of Natural Resources of the Russian Federation, Ekaterinburg (in Russian)